

## **The 2022 Canadian Society for Pharmaceutical Sciences/Canadian Chapter of Controlled Release Society Annual Symposium was held virtually from June 1-2, 2022.**

On June 1st, the focus was on trainees as part of the Pharmaceutical Sciences Trainee Day which included student-focused workshops, panel discussions and oral presentations from trainees as part of our annual poster competition. In the afternoon Professor Pieter Cullis of UBC presented his CSPA Life Time Achievement Award lecture “From Basic Research to COVID-19 mRNA Vaccines: The Lipid Nanoparticle Story”.

On June 2nd, the key theme was Driving Beyond the Pandemic: Innovation and Paradigm Shift in Regulatory Sciences. The agenda was packed with speakers from Health Canada as well as health and pharmaceutical industry leaders. Key discussions included how regulation modernization is accelerated to meet pandemic needs which evolve into adaptation of agile regulations, and its impact on future preparedness to bring preventative and curative treatments to Canadians. The goal was to create a dynamic environment for regulatory agency, industry, and academia to effectively interact to ensure the future well-being of Canadians.

Abstracts of the presentations by the meeting participants were as follows:

### **BIOMEDICAL SCIENCES**

#### **Development of three-dimensional myocardium as an alternative to heart transplant**

Farinaz Ketabat,<sup>1</sup> Titouan Maris,<sup>1</sup> Zahra Yazdanpanah,<sup>1</sup> Nicole Sylvain,<sup>2</sup> Huishu Hou,<sup>3</sup> Michael Kelly,<sup>3</sup> Xiongbiao Chen,<sup>4</sup> Ildiko Badea,<sup>5</sup>

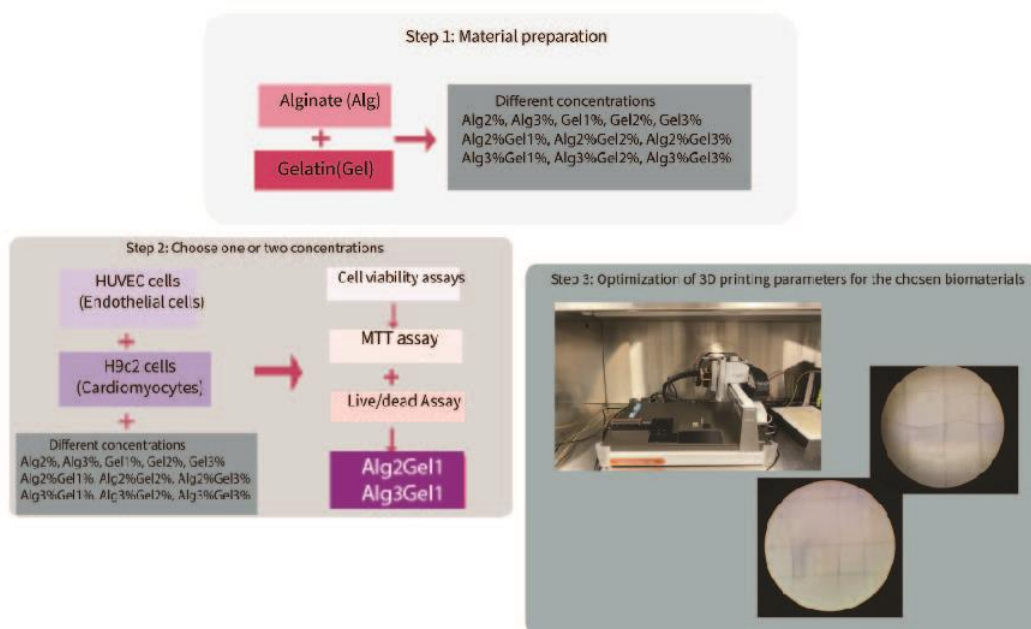
<sup>1</sup>Division of Biomedical Engineering, University of Saskatchewan, SK, Canada, Saskatoon, Canada

<sup>2</sup>Clinical Trials Support Unit, College of Medicine, University of Saskatchewan, SK, Canada, Saskatoon, Canada;

<sup>3</sup>Department of Surgery, College of Medicine, University of Saskatchewan, SK, Canada, Saskatoon, Canada;

<sup>4</sup>Division of Biomedical Engineering, University of Saskatchewan, SK, Canada; Department of Mechanical Engineering, College of Engineering, University of Saskatchewan, Saskatoon, Saskatchewan, Canada; <sup>5</sup>Drug Discovery and Development Research Group, College of Pharmacy and Nutrition, University of Saskatchewan, Saskatoon, Saskatchewan, Canada

**Purpose:** Limited capacity of heart tissue to regenerate itself is one of the main reasons why myocardial infarction (MI) becomes a progressively debilitating disease that cannot be stopped by pharmacotherapy (1-3). The goal of myocardial tissue engineering (MTE) is to provide a microstructure mimicking the microenvironment of the myocardium by replacing the infarcted area (4). We designed 3D-printed scaffolds to mimic the microstructure of the myocardium for MTE applications. **Methods:** Two natural polymers, alginate and gelatin, were selected as components of 3D-printed scaffolds. Various concentrations of the polymer solutions (1-3% w/w) were prepared. The viability of cardiomyocytes and endothelial cells was studied through MTT assay and Live/Dead assay 3D-printing parameters were optimized for the polymer combinations supporting the highest cell viability to print the scaffolds with a specific layout, mimicking myocardium architecture i.e., fibre alignment of the heart with optimal endothelial-cardiomyocyte cell-to-cell distance to provide oxygen and nutrients to cardiomyocytes. Cell viability of the 3D-printed and their mechanical properties were assessed. **Results:** Of 11 different concentrations, alginate 2 %-gelatin 1 % (Alg2Gel1) and alginate 3 %-gelatin 1 % (Alg3Gel1), which showed the highest cell viability (approximately 100%), were selected for optimizing the 3D-printing parameters. The scaffolds of Alg3Gel1 with strand diameters of 100 and 150  $\mu$ m and infill distance of 1.5 mm resulted in the best printability and fidelity. Regarding Alg2Gel1, the strand diameter of 200  $\mu$ m and infill distance of 1 mm led to fabricating 3D scaffolds with high printability and fidelity. The elastic moduli of the 3D-printed scaffolds were approximately 35 kPa, comparable to that of human native myocardium (10-15 kPa). **Conclusion:** the 3D-printed scaffolds provided growth support for cardiomyocytes and endothelial cells. These scaffolds will be engineered to induce vascularized myocardium tissue in vitro and in vivo.



## Theophylline formulation inhibits oxidative damage activation and may ameliorate OVA-Induced Allergic Airway Inflammation in Mouse Balb/c Model

David Calderon Guzman, Ernestina Hernandez Garcia, Norma. Osnaya Brizuela, Maribel Ortiz Herrera, Armando Valenzuela Peraza, Gerardo Barragan Mejia

Instituto Nacional De Pediatria, Mexico, Mexico

**Purpose.** Asthma, a global public health issue, seriously affects the life quality of children. Theophylline, a phosphodiesterase inhibitor, is a drug that has been employed in treating respiratory diseases. Currently, the limitation in the use of theophylline in children is the lack of good pharmaceutical formulation. **Methods.** We studied the protective effects of a novel theophylline formulation on asthma induced, particularly the action on airway inflammation and on the modulation of select oxidative stress biomarkers in a standard experimental asthma model, using ovalbumin sensitized Balb/c mice. Mice was decapitated after the latest administration of the treatment and their cerebrum were immediately dissected and submerged in a solution of NaCl 0.9% and maintained at 4°C. Besides, blood samples were obtained and used to asses the levels of hemoglobin and triglycerides. Each brain and lunge was homogenized in 3ml of tris-HCl 0.05M pH 7.2 and used to assay lipoperoxidation and Glutathion levels determination using previously validated methods. **Results.** The theophylline significantly inhibited Ova-induced mucus production and inflammatory response, and considerably impaired Ova-induced generation of reactive oxygen species. The above results suggest that the theophylline oral formulation relieves asthmatic airway inflammation. **Conclusion.** We believe that this involves oxidative stress-responsive lipid peroxidation pathway; thus, highlighting its potential as a useful therapeutic agent in the management asthmatic children. Besides, histological changes revealed lesions of lung cells in experimental animals treated with ovalbumin.

## **Protective Effects of Pyrroloquinoline Quinone in Folate-Deficient Glial Cells**

Vishal Sangha,<sup>1</sup> Qing Rui Qiu,<sup>2</sup> Reina Bendayan,<sup>3</sup>

University of Toronto, Toronto, Canada

**Purpose:** Folates (Vitamin B9) are critical in several biosynthetic processes, with transport mediated by three major pathways: folate receptor alpha (FR $\alpha$ ), proton-coupled folate transporter (PCFT), and reduced folate carrier (RFC)<sup>1</sup>. Brain folate transport primarily occurs at the blood-cerebrospinal fluid barrier (BCSFB) through concerted actions of FR $\alpha$  and PCFT, with impairments in this transport resulting in the pediatric neurological disorder cerebral folate deficiency (CFD)<sup>1</sup>. To identify novel treatment strategies for CFD, we have identified the functional upregulation of RFC by nuclear respiratory factor 1 (NRF-1) at the blood-brain barrier, once indirectly activated by the natural compound pyrroloquinoline quinone (PQQ)<sup>1</sup>. PQQ is also of interest due to its anti-inflammatory, antioxidant, and mitochondrial biogenesis effects<sup>2</sup>. In this study, we examined inflammatory and oxidative stress responses in vitro, in mixed glial cells in the context of folate deficiency, and PQQ's role in reversing these effects. **Methods:** Primary cultures of mouse mixed astrocytes and microglia grown in a folate-complete media (control) or media lacking folic acid (folate-deficient condition) were treated with 5  $\mu$ m PQQ (or DMSO vehicle) for 24 or 48 hours. Following treatment, cells were collected for qPCR analysis to examine changes in gene expression of several inflammatory and oxidative stress markers. **Results:** Gene expression of the inflammatory markers IL-1 $\beta$ , IL-6, CCL3, CXCL10, and the oxidative stress marker iNOS were significantly increased in folate deficient conditions compared to control, with PQQ treatment (24 and 48 hours) leading to significant decreases in expression of these markers compared to vehicle. **Conclusion:** These results demonstrate the effects of folate deficiency in inducing glial inflammatory and oxidative stress responses, which may contribute to the neurological deficits seen in CFD. PQQ may represent a novel treatment strategy for disorders associated with CFD, as it can increase folate uptake, while in parallel reversing many abnormalities associated with brain folate deficiency.

## **Computational Modeling to Predict the Interactions of Different Aryl Hydrocarbon Receptor Modulators Bound to its PAS-B Domain**

Farag Mosa, Ayman. El-Kadi, Khaled Barakat

Pharmacy and Pharmaceutical Sciences, University of Alberta, Edmonton, Canada

**Purpose:** The aryl hydrocarbon receptor is an environmental sensor that integrates metabolic and biological signals to control complicated cellular responses. It regulates numerous genes' expression and plays a pathophysiological function in several diseases, including cancer progression and cardiovascular diseases. The full-length AhR comprises several domains, including bHLH, PAS-A, PAS-B, and transactivation domains. The PAS-B domain plays a crucial role in interacting with small molecules via its ligand-binding domain (LBD). Here, we used a combination of computational algorithms to construct 3-dimensional (3D) structures of the PAS-B domain in human and mouse to understand the interactions of AhR with various AhR ligands (agonists/antagonists). **Methods:** The available AhR crystal structures lack the PAS-B domain. Hence, we used homology modeling tools to build the (3-D) structure of the PAS-B domain. Two PAS-B models were selected and validated using molecular dynamics (MD) simulations, followed by clustering analysis to extract their most dominant conformations. A set of AhR ligands were then docked to the identified dominant conformations of each model. The docked complexes were then relaxed using a second round of MD simulations. The binding free energy of each compound was then calculated using the MM-PBSA method. **Results:** The 3D structures of the human hypoxia-inducible factors (HIF-2 $\alpha$  and HIF-1 $\alpha$ ) were used as templates. Clustering analysis extracted the dominant conformations from the constructed models. Molecular docking for AhR ligands explored up to 3000 poses and the top 30 poses with the highest docking scores were selected for final analysis. Each ligand-protein

complex was then subjected to a 50 ns of classical MD simulation, followed by MM-GBSA calculations. Conclusion: The modes of action of AhR ligands were predicted, demonstrating the essential residues that interact with AhR. Our work paves the way towards developing novel AhR antagonists to treat various diseases mediated by AhR signaling.

### **Myeloperoxidase-mediated toxicity of the industrial contaminant, 6-PPD, in vitro**

Yiheng Liu, Arno Siraki, Dinesh Babu, Béla Reiz, Lusine Tonoyan

Faculty of Pharmacy & Pharmaceutical Sciences, University of Alberta, Edmonton, Canada

**Purpose** A product of the industrial contaminant, 6-PPD (N-[1,3-Dimethylbutyl]-N'-phenyl-p-phenylenediamine), has been recently reported as highly toxic to coho salmon and potentially toxic to other aquatic organisms<sup>1</sup>. The potential toxicity of 6-PPD in humans, however remains unknown. The enzyme myeloperoxidase (MPO) in neutrophils, is known to produce free radical and oxidized metabolites from xenobiotics and so its role in 6-PPD-mediated toxicity was investigated. Methods UV-visible spectroscopy and liquid chromatography-mass spectrometry (LC/MS) were performed to investigate the MPO mediated oxidation of 6-PPD and identify possible metabolites in the absence/presence of glutathione (GSH). 6-PPD's cytotoxicity in HL-60 cell line, a MPO-rich human leukemia cell line, was assessed with Cell-TiterGlo® viability assay kit. Electron paramagnetic resonance (EPR) was applied to capture the possible radical products in the presence of GSH by using a radical trapping agent DMPO. Results UV-Vis analysis of MPO-catalyzed oxidation of 6-PPD demonstrated minor but detectable changes in the 6-PPD spectrum, whereas the addition of GSH resulted in greater spectral change indicating a possible GS-6-PPD conjugate formation which significantly increased in the presence of H<sub>2</sub>O<sub>2</sub> (the endogenous cofactor for MPO). LC/MS showed the formation of multiple products, including the possible GS-6-PPD conjugates, and N-dealkylated metabolites which could potentially induce cytotoxicity. The IC<sub>50</sub> of 6-PPD treated in HL-60 cells for 24 h was 2.039 μM. EPR data of MPO-mediated 6-PPD oxidation showed a concentration-dependent relationship between 6-PPD and GS radical signal intensity in the presence of H<sub>2</sub>O<sub>2</sub>. Conclusion 6-PPD's oxidation can induce radical products formation and GSH conjugation in the presence of MPO. Furthermore, 6-PPD induces toxicity in MPO-rich HL-60 cells. Our results suggest that MPO could be an activator of 6-PPD's toxicity in humans, particularly during inflammation. A potential relationship between 6-PPD's oxidative metabolites and toxicity mechanism requires deeper investigation to determine its toxicity in mammals, including humans.

### **Sex-Specific Differences in Rat Cardiac Cytochrome P450 levels**

Samar Gerges, Ayman El-Kadi,

Faculty of Pharmacy and Pharmaceutical Sciences, University of Alberta., Edmonton, Canada

**Purpose:** Arachidonic acid is metabolized by cardiac cytochrome P450 (CYP) hydroxylases into hydroxyeicosatetraenoic acids (HETEs), several of which are cardiotoxic, and by CYP epoxygenases into cardioprotective epoxyeicosatrienoic acids (EETs). CYP hydroxylases and cardiotoxic HETEs are significantly elevated in cardiac hypertrophy. Cardiac hypertrophy is generally less common in women than in men. Several studies have demonstrated higher vascular and cardiac levels of cardioprotective EETs in females, as opposed to higher cardiotoxic HETEs in males. Female sex hormones could lower undesirable HETEs. The aim of this study was to investigate sex-specific differences in the levels of cardiac CYP hydroxylases and epoxygenases in male and female rats. Methods: The mRNA and protein expression of several CYP enzymes were assessed in the heart of adult male and female Sprague Dawley rats by real-time polymerase chain reaction and western blot techniques, respectively. Results: We found significant sex-specific differences in the levels of several cardiac CYP enzymes.

At the mRNA level, the CYP epoxygenases 2J3 and 2C11 were significantly higher in female rats compared to male rats, while 2C23 was significantly higher in male rats compared to female rats, and CYP1B1 showed no significant difference. At the protein level, CYP1B1 and CYP2J showed no significant difference between the two sexes. The CYP hydroxylases 4A and 4F were found to be significantly higher in female rat hearts compared to male hearts at both mRNA and protein expression levels. Conclusion: We showed significant sex-specific differences in the expression levels of different CYP enzymes in the heart, which could in turn affect the levels of their metabolites and thus affect the development and/or the progression of cardiac hypertrophy. This work was supported by a grant from the Canadian Institutes of Health Research [CIHR PS 168846] to A.O.S.E-K. S.H.G. is the recipient of Alberta Innovates Graduate Student Scholarship.

### **Measuring the Activity of Histone Lysine Methyltransferases in Enzymatic Assays Using LC-MS/MS** Olufola. Ige, Wenxia Luo, Thordur Hendrickson-Rebizant, Ted Lakowski,

University Of Manitoba, Winnipeg, Canada

**Purpose** Histone lysine methyltransferases (HMTs) are one branch of the epigenetic control of gene expression. Aberrations in such methylation are involved in cancer. We developed an LC-MS/MS method to quantify HMT activity using recombinant SET domain-containing lysine methyltransferase 7/9 (SET 7/9) as a representative HMT and its substrate histone H3. Such methods can determine the enzyme kinetics of HMT in advance of the development of HMT inhibitors. **Method** An LC-MS/MS method was developed to quantify methyllysines from hydrolyzed methylated histones using stable isotope labeled lysine as an internal standard. SET7/9 and histone H3 were expressed in E coli. SET7/9 was purified using immobilized metal affinity chromatography. Histone H3 was refolded from inclusion bodies and purified using HPLC. Enzymatic reactions were prepared in a volatile buffer with S-Adenosyl-L-methionine (AdoMet) and histone H3 substrates. The linearity of the reaction the pH optimum and  $V_{max}$  and  $K_M$  values for each substrate were determined. **Results** Using the LC-MS/MS method we found that the pH optimum for SET7/9 is 9. We confirmed that the enzyme is only capable of producing monomethyllysine (MML) under a wide variety of conditions. The enzymatic rate of reaction was linear up to 200 nM of SET7/9 and was linear up to 60min at fixed enzyme and substrate concentrations. The  $V_{max\ app}$ ,  $V_{max}$  and  $K_{M\ app}$  and  $K_M$  were determined for AdoMet and histone H3. The data suggests that the enzyme follows a sequential substrate binding and product dissociation mechanism. **Conclusion** The LC-MS/MS method was capable of measuring HMT activity over a wide range of methyllysine concentrations and heavy lysine was an effective IS. The method is appropriate for enzyme activity experiments as well as for HMT inhibitor assays.

### **Cross-serotype analysis of drug binding interactions in the conserved $\beta$ -OG site of Dengue virus envelope protein: a computational approach**

Minwoo Ha, Farag Mosa, Khaled Barakat,

University of Alberta Faculty of Pharmacy and Pharmaceutical Sciences, Edmonton, Canada

**Purpose:** Dengue virus (DENV) is a flavivirus with four serotypes that cause hemorrhagic disease, presenting a global health burden. A conserved druggable site, termed the  $\beta$ -octylglucoside ( $\beta$ -OG) site, has been identified at the hinge of the envelope (E) protein1. Small-molecule binding of this site blocks viral replication2, presenting an avenue for drug discovery. Through an in silico approach, this study aims to comprehensively characterize the binding modes of compounds that were shown to exhibit in vivo viral inhibition. **Methods:** Homology modeling was used to construct a model of DENV envelope protein for each serotype using previously published crystal structures as templates. The models were verified through AlphaFold to ensure validity. After adjusting the systems to physiological conditions, 120 ns of classical molecular dynamics simulations were conducted to equilibrate the systems. Dominant conformations of the protein were extracted from these trajectories through clustering analysis. Pharmacophore analysis was performed to identify key interactions related to drug binding. Subsequently, docking simulations were performed to further elucidate the binding modes of the proposed viral

inhibitors and analyzed to characterize the free energy and hydrogen bonding present in the systems. Results: This is the first study to holistically analyze the cross-serotype binding modes of various DENV E-protein inhibitors reported in literature. Our analysis reveals a common pharmacophore profile shared by all studied ligands that can be used to further optimize future drug discovery against the  $\beta$ -OG site. Per-residue binding free energy and hydrogen bond networks are presented, revealing key residues for each serotype that are involved in ligand binding. Conclusion: In silico analysis of DENV envelope protein structures was used to define the common pharmacophore properties of inhibitors and key residue contributions to binding. This study provides a structural rationale for observed viral inhibition against DENV and serves as a basis for further drug discovery.

### **Metabolomic methods of quantifying DNA methylation and other modified DNA bases in cancer cell lines using LC-MS/MS**

Wenxia Luo, Olufola Ige, Ted Lakowski

University of Manitoba, Winnipeg, Canada

Purpose: Cytosine methylation (mdC) is a known epigenetic modification to DNA that controls gene expression, and several new DNA modifications have been discovered. Aberrant deposition of promoter mdC is associated with gastric cancer and methyl adenosine (mdA) is elevated in glioblastoma. However, no method has been developed to quantify all DNA modifications from cells and such methods are needed to develop metabolomic biomarker screens for cancer and to evaluate new treatments for cancer. We developed and validated an LC-MS/MS method to quantify 5-methylcytosine (5-mdC), 5-hydroxymethylcytosine (5-hmdC), 5-formylcytosine (5-fdC), 5-carboxycytosine (5-cadC), mdA, and the 4 canonical DNA bases from hydrolyzed genomic DNA extracted from cultured cells. Methods: The methods were developed and validated using synthetic 20mer dsDNA oligonucleotides each containing a single modified nucleotide. The oligonucleotides were enzymatically hydrolyzed into nucleosides and the free canonical and modified bases quantified using LC-MS/MS. The method was evaluated using hydrolyzed genomic DNA extracted from gastric cancer cell lines. Results: The methods were capable of quantitative recovery of the canonical and modified DNA bases from the synthetic oligonucleotides and accuracy precision and low limit of quantification were determined. We detected elevated 5-hmdC, mdA in gastric cell lines SNU 719, SNU 216, AGS treated with DNA methyltransferase inhibitors. Conclusions: The LC-MS/MS methods can quantify the total amounts of the modified bases on DNA isolated from cancer cell lines. This method will be further developed to generate metabolomic biomarker screens and to test DNA methyltransferase inhibitors on cancer cell lines.

### **Preparation and Characterization of Phenyl 4-(2-Oxoimidazolidin-1-yl)benzenesulfonate Amino Acid Salt Prodrugs as New Water-Soluble Antimitotic Agents: Proof of Principle**

Joanie Ringuette, Sébastien Fortin, Vincent Ouellette

CHU de Québec-Université Laval, Québec, Canada

Purpose: Cancer is a major global public health problem due to its frequency and mortality rate. Despite advances in treatments, cancer remains a difficult disease to treat, and new effective treatments are in great demand. To that end, Dr. Fortin and his research group have been developing for several years new anticancer agents called phenyl 4-(2-oxo-imidazolidin-1-yl)benzenesulfonates (PIB-SOs). PIB-SOs are potent antimitotic agents exhibiting antiproliferative activity in the nanomolar range, blocking the cell cycle progression in the G2/M phase and disrupting microtubules ultimately leading to the cancer cell death. However, the water solubility of PIB-SOs is low causing problems during galenic formulation and their biological evaluation. The aim of this study is therefore to design, prepare, characterize, and evaluate the water solubility of new amino acid salts of PIB-SOs. Method:

The new PIB-SO amino acid salt prodrugs were synthesized using conventional organic chemistry methods and then were purified by automated flash chromatography. They were confirmed by <sup>1</sup>H and <sup>13</sup>C NMR, melting point and HPLC-MS and they were evaluated for their water solubility using the shake-flask solubility assay. Results: At the moment, 3 new amino acid hydrochloride salt prodrugs of PIB-SOs namely 4-(2-aminoacetamido)-3-chlorophenyl 4-(2-oxoimidazolidin-1-yl)benzenesulfonate, 2-(2-aminoacetamido)-5-chlorophenyl 4-(2-oxoimidazolidin-1-yl)benzenesulfonate and 4-(2-aminopropanamido)-3-chlorophenyl 4-(2-oxoimidazolidin-1-yl)benzenesulfonate have been designed, prepared and characterized with a high degree of purity. The new amino acid hydrochloride salt prodrugs of PIB-SOs show important increased water solubility (1.2 - 1.6 mg/ml) compared to their parent PIB-SOs (< 0.01 mg/ml). Conclusion: The new PIB-SO amino acid salt prodrugs are new water-soluble antimitotic agents. The evaluation of their biological and pharmacological properties is in progress to investigate their potential in the treatment of cancers.

### **17-(R/S)-Hydroxyeicosatetraenoic acid (HETE) increases the transcription of CYP1B1 and allosterically increases its catalytic activity**

Fadumo. Isse, Ayman. El-Kadi

Faculty of Pharmacy and Pharmaceutical Sciences, University of Alberta, Edmonton, Canada

Purpose: Cardiac hypertrophy is a response to initial decreased cardiac pumping or pressure and volume overload. Previous studies conducted in our laboratory reported that cytochrome P450 1B1 (CYP1B1)-mediated arachidonic acid metabolites namely, midchain HETEs have a cardiotoxic effect and involved in the development of cardiac hypertrophy. Therefore, the objective of the current study was to investigate the effect of (R) and (S)-enantiomers of 17-HETE on CYP1B1 in adult human cardiomyocytes (AC16) and their subsequent role in the development of cardiac hypertrophy. Methods: AC16 cells were treated with an increasing concentration of (R) and (S)-enantiomers of 17-HETE for 24 h. The CYP1B1 was assessed at the mRNA, protein, as well as catalytic activity levels using real-time polymerase chain reaction, western blot and EROD assay, respectively. Cardiac hypertrophy was also assessed by measuring the level of expression of the cardiac hypertrophic markers. Results: Cells treated with 20 μM of R- and S- enantiomers of 17-HETE significantly increased the CYP1B1 gene expression (p < 0.001). This was correlated with a significant increase in CYP1B1 protein expression in AC16 cells treated with (R)- and (S)- 17-HETE (p, 0.03 and 0.04, respectively) in comparison to control. Interestingly, the catalytic activity of human recombinant CYP1B1 was significantly increased by (R) and (S)-17-HETE. In addition, (R) and (S)-17-HETE treatment significantly increased the expression of the cardiac hypertrophic markers such as atrial natriuretic hormone (ANP), and β/α-myosin heavy chain in AC16 cells. Conclusion: Our results provide the first evidence that (R)- and (S)-17-HETE increases the CYP1B1 mRNA and protein levels at the transcriptional level and the CYP1B1 catalytic activity in human recombinant CYP1B1 through allosteric mechanism. Acknowledgment: This work was supported by the Canadian Institutes of Health Research [CIHR PS 168846] to A.O.S.E.

### **The Oxidation of Arylamine Fenamate Compounds by Neutrophil Myeloperoxidase Produces Toxic Reactive Metabolites**

Newton Tran, Dinesh Babu, Lusine Tonoyan, Arno Siraki

Faculty of Pharmacy & Pharmaceutical Sciences, University of Alberta, Edmonton, Canada

Purpose: The interactions between peroxidase enzymes and fenamic acid-like NSAIDs cause the formation of reactive oxygen species, potentially leading to toxic side-effects. The aim of this study was to investigate the bioactivation of arylamine fenamate compounds based on N-phenylanthranilic acid (NPA) and four drug analogues: flufenamic acid (FFA), mefenamic acid (MFA), meclofenamic acid (MCLOFA), and tolfenamic acid

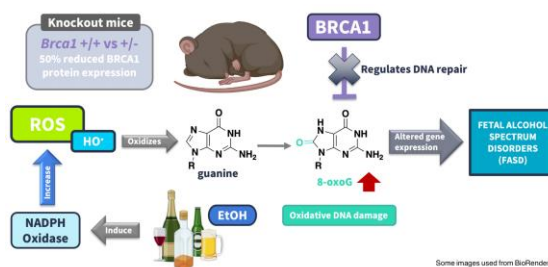
(TFA) via myeloperoxidase (MPO). The heme enzyme MPO is known to catalyze oxidation reactions of numerous xenobiotics into reactive metabolites. It is hypothesized that the enzymatic oxidation of these arylamine fenamate compounds by MPO will result in reactive metabolites that lead to cell toxicity in leukemia cells. Methods: To test our hypothesis, we used biochemical approaches where purified MPO from human neutrophils was used for UV-vis spectrophotometry, liquid chromatography-mass spectrometry (LCMS), and electron paramagnetic resonance (EPR). In addition, *in vitro* studies were performed with HL-60 promyelocytic leukemia cells, which are high in MPO content, to analyze the cytotoxic potential of these reactive metabolites. Results: In UV-vis spectrophotometry studies, it was observed that MPO catalyzed the oxidation of most fenamate compounds, but not NPA. All fenamate compounds demonstrated MPO-catalyzed cytotoxicity in HL-60 cells, where the most and least toxic compounds were observed to be MCLOFA and NPA, respectively. Furthermore, LCMS analysis of the oxidized products displayed the formation of dimers, hydroxylated, and quinoneimine species, although, glutathione (GSH) conjugates were only detected for MFA and TFA. EPR spin trapping with 5,5-dimethyl-1-pyrroline-N-oxide (DMPO) using reduced GSH revealed that all fenamate compounds resulted in the formation of glutathionyl radicals ( $\cdot$ SG) in a linear concentration-dependent manner, with the highest and lowest  $\cdot$ SG signal response being MCLOFA and FFA, respectively. Conclusion: These findings revealed a correlation between reactive metabolite reactivity and cytotoxicity of arylamine fenamate compounds mediated by the oxidation of MPO.

## Ethanol-initiated oxidative DNA damage in Brca1 knockout mice

Vivien Trinh, Kian Afsharian, Peter Wells

Leslie Dan Faculty of Pharmacy, University of Toronto, Toronto, Canada

Purpose: Breast cancer 1 protein (BRCA1) regulates DNA repair and protects the fetal brain from the DNA lesion, 8-oxoguanine (8-oxoG), which is caused by reactive oxygen species (ROS). 8-OxoG contributes to neurodevelopmental disorders like fetal alcohol spectrum disorders (FASD). Our lab previously characterized a Brca1 knockout (KO) mouse model whereby heterozygotes (+/-) exhibit over a 50% reduction in BRCA1 compared to their wild-type (++) littermates. Herein, we determined the time course for 8-oxoG formation in fetal brains exposed *in utero* to the ROS-enhancing drug ethanol (EtOH) or saline vehicle. Methods: Heterozygous Brca1 KO mice were mated, and pregnant dams were treated intraperitoneally with 4 g/kg EtOH or saline vehicle on gestational day 17. EtOH-exposed dams were sacrificed at 3, 6, or 9 hours post-treatment, and saline-treated dams immediately or at 6 h. Fetuses were extracted and genotyped. Brain DNA was extracted and 8-oxoG was quantified using ELISA. Results: Compared to 8-oxoG in fetal brains at 0 h following maternal saline injection, there was about a ~30% increase at 6 h following saline injection and ~87% increase at 6 h following EtOH injection. 8-OxoG in EtOH-exposed Brca1 +/- fetal brains was ~20% higher than in Brca1 +/- brains at 3 h, and ~10% higher at 6 h. No sex differences were observed. Conclusion: The 6 h time of maximal 8-oxoG formation in both EtOH- and saline-exposed fetal brains will be used in future studies of oxidative DNA damage. Maternal saline injection may increase 8-oxoG by enhancing fetal ROS-producing NADPH oxidase enzymes. Genotypic differences in fetal brains confirm a protective effect of BRCA1 against oxidative DNA damage.





## **Investigating the anti-atherosclerotic effects of a cyclic azapeptide, MPE-298, ligand of CD36/SR-B2 in hypercholesterolemic apolipoprotein E-deficient mice**

Jade Gauvin, Sylvie Marleau,

University of Montreal, Faculty of Pharmacy, Montreal, Canada

Purpose CD36, a class B2 receptor scavenger expressed by monocytes/macrophages, is at the crossroad of lipid metabolism and innate immune response. In particular, it is known to play a key role in the development and pathogenesis of atherosclerosis. To investigate CD36/SR-B2 as a potential therapeutic target in atherosclerosis, Synthetic azapeptide derivatives of GHRP-6 were developed which exhibited high selectivity for CD36. The present study aimed to assess the anti-atherosclerotic potential of MPE-298 (Ala-AzapropargylGly-D-Trp-Ala-Trp-D-Phe-Lys(allyl)-NH<sub>2</sub>), a potent macrocyclic azapeptide ligand of CD36, exhibiting anti-inflammatory activity in cell-based screening assays. Methods. Male apolipoprotein E deficient (apoE<sup>-/-</sup>) mice were fed a high fat high cholesterol (HFHC) diet containing 1.25% cholesterol (D12108, Research Diets, USA), from 4 weeks of age. Mice were treated by daily subcutaneous injections of 300 nmol MPE-298/kg or the linear MPE-003 azapeptide (positive control) or vehicle (0.9% NaCl), from 12 to 20 weeks of age, with 11-12 mice in each group. The effect of treatment on aortic lesion progression was assessed by en face analysis of aortic crosses. Oil Red O-stained lesion areas were analyzed with computer-assisted planimetry. Necrosis was assessed by image analysis and plasma cytokines were assayed using commercial ELISA kits. Results. The results show that, compared to the vehicle-treated group, MPE-298 reduced aortic arch lesion progression by 40% (p<0.0001), which is similar to the reduction obtained with the positive control group (42%). A similar tendency for lesion reduction was observed in brachiocephalic arteries (BCA), whereas necrotic areas in aortic sinuses were diminished by 24% (p<0.05). A 53% reduction of IL-1β (p=0.04) and of TNFα by 43% (p=0.03) plasma levels were observed in MPE-298 mice compared to vehicle-treated apoE<sup>-/-</sup> mice. MPE-298 did not modulate plasma cholesterol levels. Conclusion. The macrocyclic azapeptide MPE-298 reduced atherosclerotic lesion progression. These effects were associated with anti-inflammatory activity and increased sinus lesion stability.

## **Assessing the potential impact of vape additives on lung surfactant model systems**

Nic Van bavel, Elmar Prenner, Raimar Loebenberg, Patrick Lai

University of Calgary, Calgary, Canada and Faculty of pharmacy and pharmaceutical sciences, University of Alberta, Edmonton, Canada

Purpose: Use of tetrahydrocannabinol (THC)-containing e-cigarettes has been linked to severe respiratory issues, including respiratory failure [1]. The mechanism behind e-cigarette/vape-use associated lung injury (EVALI) is unclear, however, probable causative agents have been identified. Vitamin E acetate and THC were found in the lung fluid of 94% of patients [2]. Other vape additives that share similar chemical properties (vitamin E and cannabidiol (CBD)) are commonly found in the same products. One potential target for these additives is lung surfactant (LS). This is a lipid-protein monolayer responsible for reducing surface tension in alveoli. This ensures proper gas exchange and stabilizes alveolar sacs against collapse during respiration. The additives lipophilic properties enable them to incorporate into LS and disrupt proper function, potentially leading to the respiratory issues associated with EVALI. Methods: We have developed a lung surfactant model system, comprised of the most prominent phospholipids found within, to investigate the impact of these additives. Surface pressure-area isotherms were measured for the model system to assess film stability, while Brewster angle microscopy was used to visualize potential changes to the lateral organization in real time. Model films with and without the additives were cycled between low and high pressures to mimic breathing cycles. Results: Results show a potential for

additives to destabilize the films, presumably by material transfer into the subphase. This effect was seen to the greatest extent in the presence the cannabinoids. Vaping additives also exhibited the capability to reduce compressibility, induce loss of material upon cycling, and interfere with lipid domain organization. Vitamin E displayed the largest effects on domain formation and size, while mixtures with cannabinoids greatly reduced domain uniformity and promoted demixing in certain cases. Conclusion: The biophysical changes observed may contribute to reduced respiratory function and provide insight into a potential mechanism for EVALI, based on the additives interference with proper lipid function.

## **Computational approaches towards the rational design of rescue drugs for hERG mutations**

Sara AlRawashdeh, Khaled Barakat

University of Alberta, Edmonton, Canada

**Purpose:** The human ether-a-go-go-related gene 1 (i.e. hERG) potassium channel is an important off-target protein for many drugs. These unwanted hERG–drug interactions can lead to life-threatening arrhythmias and other cardiac disorders, notably long QT syndrome. Over the last decades, binding of drugs to the hERG channel has led to the withdrawal of many drugs that have made it already to the market. In addition to this drug-mediated toxicity, hERG mutations can also lead to multiple channelopathies complications, including neurological, cardiac, muscular, systemic, and other serious health disorders. Therefore, a molecular-level understanding of hERG physiology, dynamics, and the impact of hERG mutations on its function is of the utmost biomedical significance. The objective of this research is to use computational modeling to study the effects of hERG mutations on the channel’s transport to the cardiomyocytes’ membrane. **Methods:** The available cryo-EM structure of the hERG channel was used as a starting point to model the full-length protein. Molecular dynamics (MD) simulations were then used to study the effects of different reported hERG type II mutations on the mechanisms of channel transport and trafficking. We specifically focused on mutations in the hERG PAS domain that were reported as type II trafficking deficient mutations e.g. G53R, E58K, T65P, and I96T. All studied hERG systems were constructed by embedding them in lipid membranes and surrounding them with water molecules at their physiologically-relevant ionic concentrations. **Results:** MD simulations of the wild type and mutated channel revealed key structural changes induced by mutations. These changes can have an effect on hERG folding and on its interactions with the different chaperone proteins. **Conclusion:** This work aimed to study mutations that have been reported to produce trafficking-deficient hERG channels. Our computational modeling unveils the key structural details behind hERG misfolding leading to its inability to be transported as a result of these mutations.

## **Investigating a Class of Polyunsaturated Fatty Acids as Potential Inhibitors of SARS-CoV-2 Host Cell Entry**

Lilian Toma, Praveen Nekkar Rao

School of Pharmacy, Health Sciences Campus, 200 University Ave. West, University of Waterloo, Waterloo, Canada

**Purpose:** Coronavirus disease 2019 (COVID-19) made a devastating worldwide impact, and new variants of severe acute respiratory syndrome virus 2 (SARS-CoV-2) continue to surface. SARS-CoV-2 initiates cell entry through binding of its Spike protein to human angiotensin converting enzyme 2 (ACE2). (1) The aim of this study was to investigate the ability of polyunsaturated fatty acids to inhibit SARS-CoV-2 Spike receptor binding domain (RBD) and ACE2 binding. **Methods:** Molecular docking studies (BIOVIA Discovery Studio) were conducted to investigate the interactions of the fatty acids at the binding interface (PDB ID: 6LZG). Enzyme-linked immunosorbent assays (ELISA) (Cayman Chemical) were used to investigate ACE2/Spike-S1-RBD binding

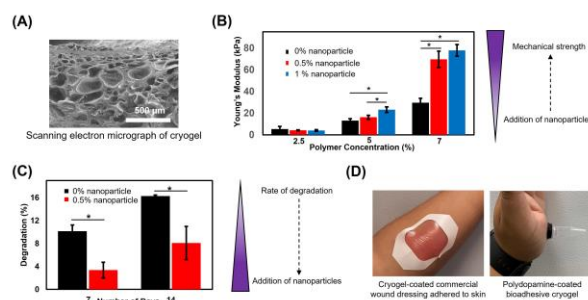
inhibition by the fatty acids at 10, 25, and 50  $\mu\text{M}$ . Human ACE inhibition activity by the fatty acids (1, 5, 10  $\mu\text{M}$ ) was measured using an ACE inhibitor assay kit (BPS Bioscience). To investigate toxicity of the fatty acids, Calu-3 (human lung adenocarcinoma) cells were treated with the fatty acids (10 & 25  $\mu\text{M}$ ) for 24 hours, and quantified with cell-counting kit 8 (Dojindo). Results: The molecular docking studies showed a trend of hydrogen bonding between the fatty acids with Lys353 (ACE2), a main virus-binding hotspot. (2) In the ELISA assay,  $\alpha$ -linolenic acid significantly reduced ACE2/Spike-S1-RBD interactions (20% inhibition at 50  $\mu\text{M}$ ,  $p < 0.05$ ), whereas oleic acid and linoleic acid exhibited weaker inhibition ( $< 10\%$  at 50  $\mu\text{M}$ ). In the ACE inhibition assay, no fatty acids significantly inhibited ACE at 1, 5, and 10  $\mu\text{M}$  (inhibition range: 0-2%). The fatty acids did not show significant toxicity to Calu-3 cells at 10 and 25  $\mu\text{M}$  (cell viability range: 93-125%). Conclusion: The results of these studies suggest that the fatty acids tested have potential in preventing SARS-CoV-2 Spike and ACE2 interactions. Additional studies are underway to obtain structure-activity data which will be useful for designing novel viral entry inhibitors.

## Tough bioadhesive nanoparticle-incorporated gelatin-based cryogels for biomedical applications

Aishik Chakraborty,<sup>1</sup> Settimio Pacelli,<sup>2</sup> Arghya. Paul,<sup>1</sup>

<sup>1</sup>Department of Chemical and Biochemical Engineering, The University of Western Ontario, London, ON, Canada, London, Canada; <sup>2</sup>Department of Biomedical Engineering, The University of Texas at San Antonio, San Antonio, Texas, USA, San Antonio, United States

**Purpose:** Natural hydrogels are suitable for biomedical applications as they are biocompatible and can mimic the native tissue environment. However, they are mechanically weak and contain small pores, which affects cell infiltration. To address these issues, we have prepared a mechanically robust nanocomposite gelatin-based scaffold containing macropores. **Methods:** Fabrication. Methacrylated gelatin was chemically crosslinked at sub-zero temperatures to form the cryogels. Nanosilicates were added to the prepolymer to enhance their mechanical strength. **Characterization.** A dynamic mechanical assay was performed to evaluate the strength of the designed cryogel. Rheological assays were conducted to further establish their mechanical resilience. The macroporous morphology of the cryogels was observed by scanning electron microscopy. Their cytocompatibility was determined using human-derived endothelial and red blood cells. Finally, the bioadhesivity of the cryogels was enhanced by coating them with polydopamine. **Results:** Energy-dispersive X-ray and Fourier transform infrared spectroscopy proved the presence of nanosilicates in the fabricated cryogel. Incorporating 0.5% nanosilicates into a 7% gelatin-laden cryogel formulation increased Young's modulus from 30 kPa to 70 kPa. The nanoparticles also reduced the rate of degradation from 16% to 8% after placing the cryogels in aqueous media for two weeks at 37 °C. The versatility of the fabrication strategy and the designed material was also proven by coating commercially available wound dressings with the cryogel. **Conclusion:** Nanosilicates increased the stiffness of natural gelatin-based cryogels. Polydopamine increased the bioadhesivity of the designed cryogel. The incorporation of nanoparticles did not adversely affect the cytocompatibility of the material. Furthermore, because the designed cryogel was ~800% water-swallowable, coating commercial wound dressings with this cryogel may elevate their ability to absorb wound exudate.



## **Pharmacological Blocking of Interleukin-1 $\beta$ Signaling Pathway Reduces Amyloid-Induced $\beta$ -Cell Toxicity in Human Islets**

Mukta. Moni, Lucy. Marzban

College of Pharmacy, Rady Faculty of Health Sciences, University of Manitoba, Winnipeg, Canada

**Purpose:** Progressive  $\beta$ -cell dysfunction and death plays a key role in the pathogenesis of type 2 diabetes (T2D), leading to hyperglycemia. Formation of toxic protein aggregates named islet amyloid in pancreatic islets is an important factor contributing to  $\beta$ -cell death in T2D. Our studies have shown that amyloid formation increases production of interleukin-1 $\beta$  (IL-1 $\beta$ ) in human islets thereby promoting upregulation of Fas cell death receptor and activation of the Fas-mediated apoptotic pathway in  $\beta$ -cells. In this study, we used two pharmacological strategies, IL-1 receptor antagonist (anakinra) and IL-1 $\beta$  neutralizing monoclonal antibody (nAb), to examine if blocking IL-1 $\beta$  signaling can reduce amyloid formation and its  $\beta$ -cell toxicity as a potential strategy to preserve  $\beta$ -cells in T2D. **Methods:** Isolated human islets (n=5 donors) were cultured free-floating in CMRL medium with normal (5.5 mM) or elevated (11.1 mM) glucose (to form amyloid), without or with anakinra or nAb, for 7 days. Immunohistochemistry was performed on paraffin-embedded human islet sections for detection of insulin, amyloid (thioflavin S), and apoptosis (TUNEL). The proportion of TUNEL-positive islet  $\beta$ -cells, islet amyloid area, and amyloid-positive islets were quantified in each condition. **Results:** Human islets cultured in elevated glucose formed amyloid in a time-dependent manner whereas no or very little amyloid was detected in islets cultured with normal glucose. Treatment with either anakinra or nAb markedly reduced the proportion of TUNEL-positive (apoptotic)  $\beta$ -cells in islets cultured with elevated glucose which was associated with lower amyloid formation in anakinra- or nAb-treated islets as compared to non-treated islets cultured in the same condition. **Conclusion:** These data suggest that pharmacological blockers of IL-1 $\beta$  signaling can reduce amyloid-induced  $\beta$ -cell death in human islets. Blocking IL-1 $\beta$  signaling may provide an effective strategy to protect islet  $\beta$ -cells from amyloid toxicity and preserve  $\beta$ -cells in patients with T2D.

## **CLINICAL SCIENCES AND PHARMACY PRACTICE**

### **Quantification of Neurovasculature Changes in a Post-Hemorrhagic Stroke Animal-Model**

Olivia Perry

Memorial University of Newfoundland, St. John's, Canada

Hemorrhagic stroke (HS) encompasses 10% to 20% of all strokes [1]. Defining cerebrovascular changes associated with HS is necessary for novel pharmacological treatments. Our objective was to use high-resolution imaging technology and perfusion casting to study the neurovascular network differences in rodent brains before and after stroke to further define cerebrovascular changes. Stroke-prone spontaneously hypertensive rats (SHRsp) were divided into pre-stroke (non-stroke) controls and post-stroke (sampled after physical signs of stroke; n=53 total). At sampling, Evan's Blue (EB) Dye (30mg/kg) was infused through the femoral artery (20 minutes) prior to fixation with 4% paraformaldehyde. Vascupaint™ (MediLumine™), a bismuth vanadate latex casting compound, was then infused (1.5mL/min; 30 sec, followed by 0.7mL/min; 6 min) to opacify microvasculature. The 3D visualization of the neurovascular network was achieved using micro-Computed Tomography (micro-CT) and analyzed using bundled SkyScan 1176 Software (Bruker). Post-stroke animals exhibited EB extravasation and decreased Vascupaint perfusion macroscopically. The 3D-rendering of brains upon micro-CT imaging indicated decreased perfusion intracerebrally post-stroke. Branching and percent vascular volume analyses (considered to be affected during hemorrhage) were developed and are currently being optimized. Our study established a standardized method for the preparation, imaging and measurement of rat cerebral blood supply through use of radiopaque materials. The micro-CT images acquired demonstrate that arteries, veins and

capillaries can be perfused successfully to detect changes in neurovasculature post-hemorrhagic stroke. Our study used a novel casting compound and micro-CT technology in a unique stroke-prone animal-model for the quantification of cerebrovascular anatomy. Advances in visualization of vasculature is critical for the potential development of new treatment strategies by enabling accurate quantification of cerebrovascular supply. Further work to standardize and validate the quantification technique is necessary.

### **A Qualitative Study Examining Older Adult Usage of Complementary and Alternative Medications for Cognitive Health**

Dalya. Abdulla,<sup>1</sup> Lia. Tsotsos,<sup>1</sup> Leigh. Hayden,<sup>2</sup>

<sup>1</sup>Sheridan College, Brampton, Canada; <sup>2</sup>Healthcare Strategist, Throughline Strategy Inc., Toronto, Canada

**Purpose:** The use of complementary and alternative medications (CAM), including natural health products (NHPs), for cognitive decline and to enhance mood is well known however research guiding Older Adult patients and their caregivers to such usage is limited. To further complicate matters, health care practitioners (HCPs) are typically either unaware or unsupportive of the usage of such products among Older Adults. The purpose of this project was therefore to elucidate and understand the usage patterns of CAM and NHP products for cognitive health among Older Adults in order to construct better guidelines for HCPs regarding this usage. **Method:** A qualitative study was conducted to determine usage patterns of CAM and NHPs among Older Adults. Participants were recruited from the Center for Elder Research at Sheridan college and open-ended questions were utilized during one-on-one interviews with interested participants. **Results:** A total of 10 participants completed the interviews with an age range of 63-86 years old. Results were analyzed using the triangulation method (multiple data sources and perspectives) to identify 6 main emerging themes: fear of cognitive health decline, strategies to mitigate perceived/self-diagnosed cognitive health decline, dietary influences on cognitive health, healthcare ownership and self-care, CAM loyalty, and supporting Older Adult CAM use. Percentages of each response were also determined when identifying the themes. **Conclusion:** Results of this study show that Older Adults were extremely cognizant of their cognitive health and tended to rely on CAM and NHPs to improve any perceived declines in cognitive health. Older Adults expressed a desire for their HCPs to become better understanding of such usage and for the government to support them financially for it. Other concerns also arose regarding Older Adult awareness and perceptions of cognitive health that should be communicated to HCPs to ensure better understanding of cognitive health among Older Adults.

### **Evaluation and clinical impact of a pharmacist-led, interdisciplinary service focusing on education, monitoring, and toxicity management of immune checkpoint inhibitors**

Meagan London,<sup>1</sup> Glenn Myers,<sup>2</sup> Jonathan Stevens,<sup>3</sup> Jacqueline Richard,<sup>2</sup>

<sup>1</sup>Dalhousie University, Rothesay, Canada; <sup>2</sup>Horizon Health Network, Moncton, Canada; <sup>3</sup>Horizon Health Network, Saint John, Canada

**Purpose:**To assess pharmacist interventions and patient outcomes from a pharmacy service focused on immune related adverse event (irAE) education, irAE monitoring and irAE management in ambulatory oncology patients receiving immune checkpoint inhibitors (ICIs). **Methods:**Patients initiated on ICI(s) from 01/01/2016 to 31/08/2019 were analyzed for data collection. Part 1 summarized pharmacist interventions into 11 categories from The Moncton Hospital (TMH) cohort. Part 2 compared patient outcomes between TMH cohort and a standard of care cohort from the Saint John Regional Hospital (SJRH). Patient outcomes included emergency department visits not resulting in admission, hospitalizations due to irAE(s), ICI cycles received, treatment discontinuation due to irAE(s), completion of finite PD-1/L1 treatment course, and completion of ipilimumab. Clinical outcomes

were compared using a retrospective, matched cohort design where cohorts were matched on age (+/- 5 years), cancer diagnosis and ICI(s). Results: A total of 143 patients were included in TMH cohort encompassing 1664 pharmacist recommendations across 10 categories. The retrospective matched cohort yielded 92 matches (n = 184) with a higher odds of ICI discontinuation due to irAE(s) in the SJRH cohort (OR (95% CI) = 5.5 (1.2-24.8); p = 0.022). Conclusions: Intensive irAE education, proactive follow-up and irAE management by pharmacists results in clinically meaningful interventions which correlate to improved patient outcomes, namely, lower odds of treatment discontinuation due to irAE(s). Acknowledgements: Meagan London is a recipient of the 2022 Canadian Society of Pharmaceutical Sciences (CSPS) National Undergraduate Student Research Program Award for Dalhousie University. The authors thank Carolanne Caron for her contributions and the Canadian Association of Pharmacy in Oncology (CPhO) for funding.

### **Association between COVID-19 and mental health and coping responses of family/friend caregivers of residents in assisted living in Alberta and British Columbia**

Lauren Dayes

University of Waterloo, Kitchener, Canada

**Purpose:** This study examined coping responses to the COVID-19 pandemic used by family/friend caregivers of residents in Assisted Living (AL) facilities in Alberta and British Columbia, and the associations between these coping responses and caregiver's mental and physical health. **Methods:** An open web-based survey was administered between October 28, 2020 and March 31, 2021 to 673 primary caregivers of a resident aged 65+, who had lived in an eligible AL facility for 3+ months prior to March 1, 2020. Coping responses of interest were assessed for the 3 months following March 1, 2020. Descriptive analyses examined the distribution of caregiver characteristics. Separate modified Poisson regression models were used to estimate unadjusted and adjusted risk ratios for the associations between caregivers' mental health measures (depression and anxiety) and their select coping strategies. Multivariable models included relevant sociodemographic characteristics and considered clustering of caregivers by AL homes. **Results:** An estimated 28.6% of overall participants met the criteria for clinically significant anxiety disorder, and 38.8% met the criteria for depressive symptoms. Caregivers with depressive symptoms were significantly more likely than those without to have sought counselling (adjusted risk ratio [adjRR] = 2.18, 95% CI=1.21-3.94), started an OTC medication for sleep and/or prescription medication for anxiety or depression (adjRR = 6.13, 95% CI=3.63-10.35), started or increased their alcohol use (adjRR = 2.03, 95% CI=1.42-2.88), and started or increased their smoking or cannabis use (adjRR = 2.04, 95% CI=1.17-3.55). Similar findings were observed for associations between anxiety and coping responses. **Conclusion:** Our findings highlight the need for targeted mental health screening and resources for family/friend caregivers of AL residents, as well as further research on strategies to increase positive coping strategies for this population.

### **A Survey of Canadian Pharmacists' Knowledge and Comfort in the Management of Epilepsy and Antiepileptic Drugs**

Akshita Chandok

University of Alberta, Edmonton, Canada

**Background:** As antiepileptic drugs (AED) remain the mainstay of epilepsy management, pharmacists have the potential to play an integral role in the management. **Objective:** The goal of our study was to characterize Canadian pharmacists' knowledge and comfort in managing epilepsy and AED and identify areas of need for the development of support tools. **Methods:** An electronic survey was designed and distributed to Canadian pharmacists through professional organizations. The survey consisted of 4 sections, including demographics, knowledge, comfort, and needs assessment around epilepsy management. **Results:** A total of 605 complete responses were included. Nearly two-thirds of the participants were females (61.6%) and most reported more than



virus, protein-protein interactions. The validation of the AI analysis was performed in vitro using Calu-3 cells seeded into 96 well plates, at 40,000 cells/well. The concentration where drug toxicity occurred was determined using MTT assay. For the infection assays cells were inoculated with SARS CoV2 WA-1 strain at a 0.01 multiplicity of infection (MOI) and incubated for 60-90 minutes. The cells were provided with EMEM with 2% FBS and test compounds and incubated for additional 48 hours. Absorbance readings for each well were collected by Softmax Pro software and imported into a Microsoft Excel spreadsheet. Outliers were detected by Grubbs' test in the built-in analysis of Graphpad Prism 9. Results: This study found that, the test compounds identified as SM-4, Gefitinib, Topotecan and to a lesser extent Carfilzomib showed conventional drug-response curves, with  $IC_{50}$  values near or below that of Remdesivir with excellent confidence all above  $R^2 > 0.91$ , and no cytotoxicity at the  $IC_{50}$  concentration, in Calu-3 cells (Table 1). Cyclosporine A showed antiviral activity, but also unconventional drug-response curves and low  $R^2$  which are explained by the non-dose dependent toxicity of the compound. Additionally, Niclosamide displayed a conventional drug-response curve and good confidence, though the inherent cytotoxicity is producing an artifact antiviral efficacy Remdesivir was used as a control compound and was evaluated in parallel with the submitted test article and had conventional drug-response curves validating the overall results of the assay. Conclusions: Taken together these preliminary findings suggest that several novel compounds may have significant in vitro activity against SARS CoV2.

### **Efficacy of Potential Antiviral Therapeutics Against SARS-CoV-2 in Mice**

Adam Bess,<sup>1</sup> Frej Berglind,<sup>1</sup> Supratik Mukhopadhyay,<sup>1</sup> Michal Brylinski,<sup>1</sup> Nicholas Griggs,<sup>2</sup> Tiffany Cho,<sup>2</sup> Chris Galliano,<sup>3</sup> Kishor Wasan,<sup>4</sup>

<sup>1</sup>LSU, Baton Rouge, United State; <sup>2</sup>Trinity Consultants, Mountain View, United States; <sup>3</sup>Skymount Medical, New Orleans, United States; <sup>4</sup>University of British Columbia, Saskatoon, Canada

**Purpose:** The objective of this study was to test the in vivo efficacy of two potential antiviral therapeutics SM-4 and SM-19 identified by our Artificial Intelligence DeepDrug software against SARS-CoV-2, the causative agent of COVID-19, in the ACE2 mouse model. **Methods:** Six hours following challenge with  $5 \times 10^3$  TCID<sub>50</sub> SARS-CoV-2, human transgenic female K18-hACE2 (B6.Cg-Tg(K18-ACE2)2PrImnJ) mice were administered placebo, SM-4 at 50 mg/kg po or SM-19 50/100 mg combination once a day for 6 consecutive days at which time the animals were humanely sacrificed. The concentration of virus in lungs was determined by RT-qPCR assay. Briefly, RNA was extracted from samples stored in RNA/DNA Shield using the Quick-RNA Viral Kit (Zymo Research) according to manufacturer's protocol. RT-qPCR was performed using the following RT-PCR cycling conditions: 50°C for 15 min (RT), then 95 °C for 2 min (denature), then 40 cycles of 10s at 95°C, 45s at 62°C. Primers used for SARS-CoV-2 detection: 2019-nCoV\_N1-F 5'-GACCCCAAATCAGCGAAAT-3' 2019-nCoV\_N1-R 5'-TCTGGTACTGCCAGTTGAATCTG -3' Probe: 2019-nCoV\_N1-P: 5'-FAM-ACCCCGCATTACGTTTGGTGGACC-BHQ1-3'. Additional Experimental endpoints were also determined including body weight and body weight change and clinical chemistry determinations such as BUN, AST, and ALT. **Results:** SM-4 and SM-19 treatment resulted in a 44.2% and 42.3% reduction in lung viral load compared to non-treated placebo control respectively (Table 1). There were no significant differences in body weight and all clinical chemistry determinations evaluated (i.e., kidney and liver enzymes) between the different treatment groups. **Conclusions:** Taken together these preliminary findings suggest that these novel compounds may have significant in vivo activity against SARS CoV2 at non-toxic doses.

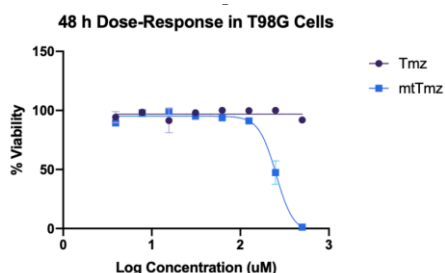
### **Peptide-Mediated Mitochondrial Delivery of Temozolomide for Evading Cellular Resistance Mechanism** Daniel Szames,<sup>1</sup> Shana. Kelley,<sup>2</sup>

<sup>1</sup>University of Toronto, Toronto, Canada; <sup>2</sup>Northwestern University, Chicago, United States

**Purpose** Temozolomide (Tmz), a DNA-alkylating agent, is currently the standard of care for the treatment of glioblastoma multiforme (GBM), one of the most lethal tumours affecting the central nervous system in adults with median survival of less than three months.<sup>1</sup> The enzyme O<sup>6</sup>-methylguanine-DNA methyltransferase (MGMT)



is responsible for removing cytotoxic lesions caused by Tmz, therefore conferring resistance to Tmz in GBM patients.<sup>2</sup> The mitochondrial genome (mtDNA) poses as a potential target for Tmz treatment, and the aim of this study is to determine if mitochondrial delivery of Tmz can evade MGMT resistance in GBM cells. Methods Our lab has developed a short peptide that can successfully penetrate the mitochondrial double membrane and localize within the mitochondrial matrix where the mtDNA is located. By synthesizing a Tmz-peptide conjugate (mtTmz), the effect of delivering Tmz to mtDNA was able to be determined using in vitro and in cellulo assays. Results mtTmz demonstrated efficient mitochondrial localization, alkylation activity, as well as an increase in potency compared to Tmz in MGMT-expressing cell lines. Mitochondrial protein analysis showed that MGMT does not localize to mitochondria in response to mtTmz-induced damage. Conclusion Delivering Tmz to mitochondria using mtTmz has shown to be more effective in treating MGMT-expressing GBM cells. These results both identify mitochondria as a potential therapeutic target in treating GBM, as well as highlight that MGMT is not responsible in the repair of mtDNA.



### Polymer-Lipid Manganese Dioxide Nanoparticles Amplify Radiation Therapy-Induced Anti-tumor Immune Response in a Syngeneic Breast Tumor Model

Ho Yin Lip, Abdulmottaleb Zetrini, Azhar Z Abbasi, Ping Cai, Andrew M Rauth, Xiao Yu Wu

University of Toronto, Toronto, Canada

Purpose: Immunogenic cell death (ICD) releases damage-associated components from dying tumor cells and plays a key role in tumor elimination by stimulating antigen-presenting cells and anti-tumor immune cells. Although radiation therapy (RT) is known to induce ICD and the abscopal effect, leading to the elimination of primary and secondary tumors, the hypoxic tumor microenvironment impairs RT and hampers cell-mediated immunity. To improve RT efficacy and enhance ICD, this work is aimed to investigate a new combination treatment using biocompatible polymer-lipid hybrid manganese dioxide nanoparticles (PLMDs) developed by our group previously. Method: Murine breast cancer EMT6 and 4T1 cells conditioned under hypoxic conditions were subjected to irradiation of various doses with or without pre-treatment with PLMDs. Clonogenic assay was used to determine cell kill. A linear quadratic model was employed to evaluate radiation responses and radiosensitization effect of PLMDs. ICD biomarkers, calreticulin (CRT), high mobility group box 1 protein (HMGB1) and ATP were assayed in vitro. Immune cell populations in orthotopic 4T1 tumor were analyzed by immunohistochemistry (IHC) following treatment of tumor-bearing mice with PLMD and RT alone or in combination. Results: PLMD+RT significantly reduced D50 compared to RT alone ( $4.57 \pm 0.27$  vs.  $7.63 \pm 0.18$  Gy in EMT6 cells and  $2.22 \pm 0.22$  vs.  $2.86 \pm 0.13$  Gy in 4T1 cells). Elevated CRT exposure, HMGB1 release and ATP secretion were observed in PLMD+RT-treated group compared to RT alone in 4T1 cells. In vivo studies using a syngeneic 4T1 tumor model revealed increased infiltration of anti-tumor CD8<sup>+</sup> T cells and CD86<sup>+</sup> macrophages, and decreased infiltration of immunosuppressive CD4<sup>+</sup> T cells and CD163<sup>+</sup> macrophages. Conclusion: The results indicated enhanced anti-tumor immune response by PLMD+RT that significantly sensitized RT under hypoxia and amplified RT-induced anti-cancer immunogenicity.

## Smart nanodiamonds as carriers for gene therapy: Introducing pH sensitivity in carrier design to modulate intracellular gene transfer by diamoplexes

Saniya Alwani, Raj Rai, Deborah Michel, Ildiko Badea

College of Pharmacy and Nutrition, University of Saskatchewan, Saskatoon, Saskatoon, Canada

**Objective:** Gene therapy require biocompatible carriers capable of transporting genetic-drugs to intracellular targets Initially we designed prototype lysyl-nanodiamonds (K-NDs) conferring a cationic surface capable of forming ‘diamoplexes’ with genes K-NDs exhibited excellent physicochemical/biological properties as a vector, however, lacked optimum transfection efficiency. Thus, histidine, a pH-modulating-moiety was introduced on K-NDs facilitate efficient gene transfer intracellularly **Methods** Histidine was covalently attached to K-NDs forming: histidyl-lysyl-NDs (HK-NDs) and lysyl/histidyl-lysyl-NDs ( $H_{50}K_{50}$ -NDs) with histidine on 100% or 50% of lysine-moieties on the ND-surface, respectively Physicochemical/biological characterizations utilized thermogravimetry, particle-size/zeta-potential measurements, electrophoresis, flow-cytometry, MTT and scanning transmission X-ray microscopy (STXM) **Results** Intracellular trafficking of diamoplexes in endo-lysosomal system and subsequent degradation of siRNA was responsible for low transfection efficiency of K-NDs. To mitigate this challenge, histidine-modified constructs were designed with surface loading of 14.49 mmoles/g histidyl-lysyl-groups. Both HK-NDs and  $H_{50}K_{50}$ -NDs produced stable colloidal dispersions, with particle size < 200 nm and zeta potential >20 mV The total amount of histidine on the surface affected gene binding and cellular level biocompatibility HK-NDs (histidine-surface-coverage=100%) formed diamoplexes at higher mass ratio ie 30:1 (ND:siRNA). Reducing histidine to 50% in  $H_{50}K_{50}$ -NDs improved effective mass ratio to 10:1 ie comparable to K-NDs Additionally,  $H_{50}K_{50}$ -NDs showed exceptional biocompatibility like K-NDs (cell-viability  $\geq 90\%$  at 500  $\mu\text{g/mL}$ ), however, HK-NDs reduced cell viability to 60-70% at 10-80  $\mu\text{g/mL}$ . Functionalization also impacted cellular-entry and exit-profile of NDs The ranking of uptake was:  $H_{50}K_{50}$ -NDs (~49%) >>K-NDs (~25%) >HK-NDs (~21%) All NDs showed cellular-exit after 5 days, leaving  $\leq 10\%$  cells with internalized diamonds. Unlike K-NDs, histidine-modified-NDs achieved a significant GFP-knockdown (an increase of 45% in GFP-negative-cells), evidencing that histidine on these constructs act as an endosomal-membrane-destabilizer, thus facilitate escape of diamoplexes to transfect anti-GFP-siRNA **Conclusion** Histidine-mediated pH-modulation renders high efficiency to diamoplexes. However, stringent balance is critical to ensure gene-binding, biocompatibility and efficient transfection **Organelle-level study of effects will illustrate design specifications for ND-based gene-therapeutics.**

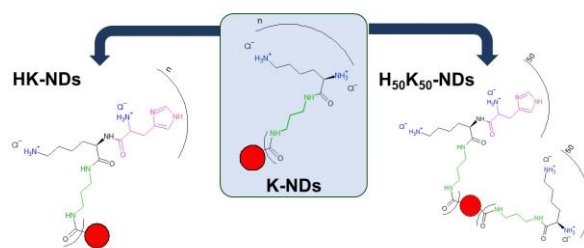


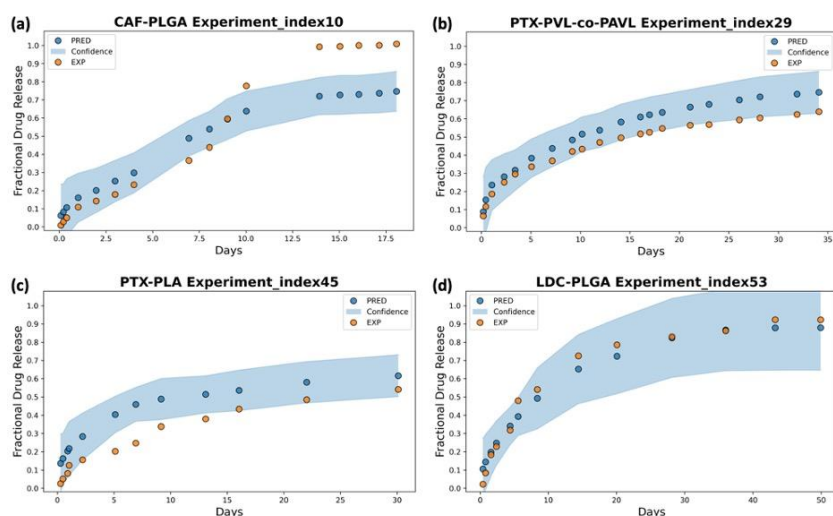
Figure 1. Histidyl-lysyl-NDs (HK-NDs) and lysyl/histidyl-lysyl-NDs ( $H_{50}K_{50}$ -NDs) at physiological pH in comparison to prototype lysyl-NDs (K-NDs)

## Towards Data-Driven Development of Polymeric Long-Acting Injectables

Zeqing Bao, Pauric Bannigan, Riley Hickman, Matteo Aldeghi, Florian Häse, Alán Aspuru-Guzik, Christine Allen

University of Toronto, Toronto, Canada

**Purpose:** Long-acting injectable formulations (LAIFs) can offer several advantages over conventional medicines, including increased bioavailability and improvements in patient compliance [1]. Several types of LAIFs have been approved for human use, including drug-loaded polymeric microparticles (MPs) [2]. Lupron Depot®, the first MP-based LAIF approved by the FDA, consists of leuprolide acetate encapsulated in poly(lactide-co-glycolide acid) (PLGA) MPs [1]. Today the majority of approved LAIFs are composed of PLGA (46%) [1]. Despite the success of PLGA-based systems they cannot be universally employed to deliver all drugs. Each drug has its own unique physico-chemical properties and drug-material interactions have a significant influence on the performance of LAIFs. Machine learning (ML) offers the ability to predict how drug-material combinations will affect final formulation properties, such as release kinetics, a priori. **Methods:** Data pertaining to 181 different drug-loaded LAIFs were extracted from previously published studies. Numerical values that described various physicochemical properties of these systems were used as ML model input features to predict in vitro drug release. Several ML models, including tree-based models, kernel-based models, and neural networks, were trained to predict drug release as a function of time and then evaluated through various model interpretation steps to excerpt learned knowledge on the drug-polymer systems. **Results:** Drug release was predicted with a high degree of accuracy using several ML model architectures. Maximum prediction accuracy was achieved using a tree-based model, which was able to not only portray drug release kinetics for a variety of drug-polymer systems a priori but also provide a measure of confidence in their predictions that was comparable to experimental uncertainty (Figure 1). **Conclusions:** The integration of ML models into drug formulation development may enable us to move away from the current trial-and-error-based approach and adopt a more efficient and sustainable formulation development process that is “data-driven”.



## Ensuring safety of polymeric nanoparticles via biodegradation and elimination studies

Amrita Dikpati, Nicolas Bertrand,

Faculty of Pharmacy, Université Laval, Quebec City, Canada

**Purpose:** Drug regulatory authorities recommend testing the toxicity and bioaccumulation of polymer excipients during pre-clinical stages of drug product development. Techniques for measuring biodegradation of nanomedicines in vivo provide information about the safety of drug carriers. Trimethyl chitosan (TMC) is a naturally abundant biopolymer that is soluble over a wide pH range (2-10), hence used as a controlled release excipient. This study was aimed at developing techniques for assessing degradation of TMC polymer and nanoparticles to produce safer pharmaceutical products. **Method:** TMC was acetylated with [3H]-acetic acid to form radiolabeled TMC. Radiolabeled TMC nanoparticles were formulated via coacervation method using

poly(ethylene glycol)-block-poly(methacrylic acid) polymer. Degradation of nanoparticles was measured using SERP (size exclusion of radioactive polymers) technique in presence of strong acid and RAW 246.7 macrophages in vitro. Wistar rats were intravenously injected with TMC nanoparticles to measure biodistribution and in vivo degradation. Finally, rats were injected with radiolabeled nanoparticles and placed in metabolic cages to measure rates of urinary and fecal excretion. Results: Labelling efficiency of [3H]-TMC was 12%. SERP was able to quantify the degradation of the polymer after incubation in concentrated acid and lysozyme. The radiolabel remained attached to degradation products after acid hydrolysis of TMC. The method could suitably monitor the degradation of nanoparticles after interactions with macrophages in culture. Lastly, after intravenous injection in rats, we affirmed that TMC nanoparticles were excreted in the urine and feces. Conclusion: The methodology could measure degradation of TMC nanoparticles, in presence of cells in culture, and in vivo. Radiolabeled TMC was excreted in urine and feces until 14 days after dosing, confirming that the polymer could be eliminated from the body after systemic administration.

### **Human Dermal Fibroblast- Derived Exosomes and application to wound healing**

Jin Wang, Emmanuel Ho

University of Waterloo, Kitchener, Canada

Purpose: Management of wound healing has been an intractable issue in regenerative medicine. More recently, cell-free therapy led by exosomes exhibits promising applications in wound closure. Exosomes are also known as remarkable carriers to transport therapeutic compounds. Here, we developed exosomes derived from human dermal fibroblasts as therapeutic agents and drug carriers. The ability of exosomes for drug delivery was studied by incorporating an anti-fibrotic drug, pirfenidone (PFD) into exosomes. The aim of this study is to evaluate the toxicity of exosomes and PFD-loaded exosomes (PFD-exosomes), and their ability to facilitate wound closure in vitro. Methods: Exosomes were harvested from human dermal fibroblasts cells and purified by affinity method. The size distribution of exosomes was determined with the NanoSight NS300. Morphology of exosomes was observed by transmission electron microscopy (TEM). PFD was incorporated into exosomes under sonication method. Drug loading efficiency was determined by ultra-high performance liquid chromatography (UHPLC). In vitro cytotoxicity of exosomes and PFD-exosomes were assessed using the MTS assay. The impact of exosomes and PFD-exosomes on the migration of fibroblasts was studied in vitro by scratch assay. Results: Purified exosomes were  $125.3 \pm 3.7$  nm in diameter when measured by NanoSight. A spherical morphology was shown by TEM.  $10.77 \pm 0.516\%$  of drug encapsulation efficiency was achieved. Both exosomes and PFD-exosomes didn't show cytotoxicity to fibroblasts. Exosomes exhibited a faster wound closure rate ( $8308 \pm 889\%$ ) than PFD-exosomes ( $67.36 \pm 7.06\%$ ) and control ( $53.62 \pm 5.57\%$ ) within 12h. Exosomes and PFD-exosomes could both achieve over 90% wound coverage 24h post wounding. We speculate that exosomes combine the benefit of facilitating wound closure as well as delivering therapeutic agents simultaneously. Conclusion: Exosomes showed promising results in enhancing wound closure without inducing cytotoxicity in vitro. Exosomes carried pirfenidone and have potential applications in scar reduction.

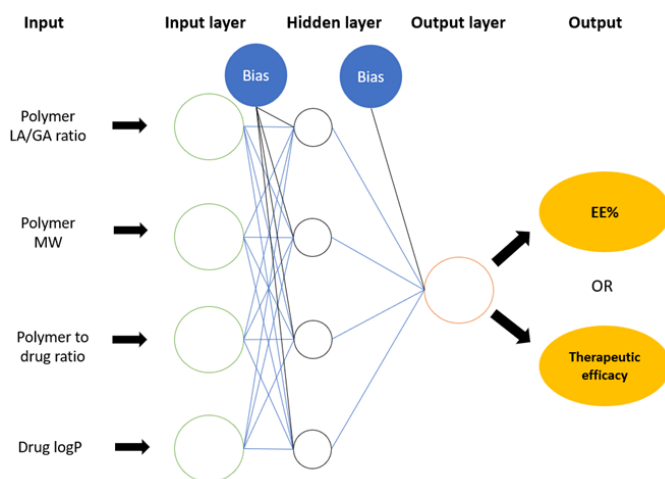
### **Machine learning-facilitated optimization of nano-drug formulations**

Sihan Dong, Emmanuel Ho

School of Pharmacy, University of Waterloo, Waterloo, Canada

Purpose: Developing nanoparticle (NP) formulations through trial and error is time-consuming and expensive. As a proof-of-concept, we will use machine learning (ML) with Python to determine the mathematical relationships

between four physicochemical properties (lactic acid to glycolic acid ratio (LA/GA), polymer molecular weight (MW), polymer to drug ratio, and drug lipophilicity (logP)) and the corresponding drug encapsulation efficiency (EE%) and therapeutic efficacy with a goal of optimizing the NP formulation compositions. Methods: In this research, three ML algorithms will be utilized to optimize poly (D, L-lactic-co-glycolic acid) (PLGA). NP formulation compositions for applications in drug delivery, including artificial neural network (ANN), partial least square regression (PLSR), and reinforcement learning (RL). Three anticancer drugs: docetaxel (DTX), doxorubicin (DOX), and carboplatin (CPT) are selected based on their different lipophilicities and ovarian cancer cell line (OVCAR-3) will serve as the model cell line. Forty-eight drug-loaded PLGA NPs with the four different physicochemical properties will be formulated and tested for their EE% and therapeutic efficacies. The data will be divided into test sets and training sets to be entered into the PLSR, ANN, and RL models, after which the models will be validated. Results: We have successfully created both PLSR and ANN models. The latter model which is shown in Figure 1 [1] consists of three main layers: the input, hidden, and output layers. To date, we have formulated CPT-loaded NPs consisting of 50:50 LA/GA PLGA with MW of 2 kDa and 5 kDa that resulted in an EE% of  $26.69\% \pm 2.17\%$  and  $12.60\% \pm 1.39\%$ , respectively, which are used as valid inputs and outputs for the programs. Conclusion: EE% and therapeutic efficacy collected from in-vitro experiments will be inputted and memorized by the computer program. Through repeated data training, the programs will be able to predict the encapsulation efficiency and therapeutic efficacy from provided NP composition details.



### **Inclusion cyclodextrin complex of cannabinoids: A promising option for improving physicochemical properties and biological performance**

Chulhun Park, Jieyu Zuo, Raimar Loebenberg

Faculty of pharmacy and pharmaceutical sciences, University of Alberta, Edmonton, Canada

Purpose: The acidic cannabinoids are naturally occurring and have recently been highlighted as potential drug candidates for treating different types of cancer. However, their anticancer activity is limited by instability and low water solubility. The objective of this study was to develop an acidic cannabinoid/cyclodextrin inclusion complex for improving the solubility and potentially biological performance of acidic cannabinoids via cyclodextrin (CD) complexation. Method: Phase solubility studies of acidic cannabinoids were performed with methylated- $\beta$ -CDs (M- $\beta$ -CD). The preparation methods of inclusion complexes were optimized by loading capacity and complexation efficiency. The inclusion complexes were characterized by solubility determination, differential scanning calorimetry (DSC), field emission scanning electron microscopy (FE-SEM). Cytotoxic effects of the acidic cannabinoid/M- $\beta$ -CD complex were performed to investigate the inhibitory effect on MCF-7

breast cancer cells after M- $\beta$ -CD complexation with each acidic cannabinoid (THCA or CBDA). Results: The aqueous solubility of THCA significantly increased to 520.3  $\mu\text{g/mL}$  as the acidic cannabinoids/M- $\beta$ -CD complexes were prepared by spray freeze drying method at the same molar ratio (1:2); this was 3-folds higher compared to those made by spray drying or freeze-drying methods. The spray freeze-drying process obtained the optimum cannabinoids/M- $\beta$ -CD inclusion complexes. Thermograms of the M- $\beta$ -CD complex showed two endothermic peaks while the characteristic peak of acidic cannabinoids was absent, indicating the successful inclusion of THCA or CBDA into the cavity of M- $\beta$ -CD. In vitro cytotoxicity studies exhibited that cannabinoids/M- $\beta$ -CD complexes had better anticancer activity than acidic cannabinoids alone. Conclusion: An improved physicochemical and physiological performance of acidic cannabinoid/M- $\beta$ -CD complexes in breast cancer cells was demonstrated. These cyclodextrin-based formulations are a promising option for optimizing the efficacy of cannabinoid delivery.

### **A Computational Study of the interaction of SHP-2 Allosteric Inhibitors: Comparing the Wildtype SHP2 to Activating Mutant SHP-2**

Maryam jama, Michael Overduin, Khaled Barakat

University of Alberta, Edmonton, Canada

Purpose: Src homology region 2 (SH2) containing protein tyrosine phosphatase 2 (SHP2) is an oncoprotein and an emerging target for cancer treatment. The overexpression of both SHP2 wildtype and its activating mutated variants are associated with developmental disorders and different malignancies such as leukemia and triple-negative breast cancer. A recent nanomolar allosteric inhibitor, SH099 stabilizes both wildtype and E76K mutant of SHP2 E76K to its auto-inhibitory conformation. However, SH099 has been reported to have a stronger affinity towards the wild type compared to the mutant protein. The objective of this research is to study the mode of binding of SH099 within the wild type and mutated SHP-2 proteins. Understanding these interactions can have implications for the therapeutic efficaciousness of SH099 in malignancies driven by E76K mutants. Methods: We used the available two co-crystallized structures of wildtype SHP2 (PDB ID 5EHR) and SHP2 E76K in complex with SH099 (PDB ID 6CRG) as starting points for molecular dynamic simulations to study their conformational dynamics. Trajectories from these simulations were used to estimate the binding affinities of the bound ligand to each protein. Further energy decomposition helped us identify the most important residues contributing to its mode of binding. Results: The SH099 binds to SHP2 E76K with a lower affinity ( $\Delta G = -354$  KJ/mol) compared to Wt SHP2 ( $\Delta G = -452$  KJ/mol). Due to the key binding regions of SHP2 E76K mutant differing from the wildtype SHP2 complex. Conclusion: The mode of binding of SH099 in both mutant and wildtype SHP2 can be explained via computational modelling. This paves the road for future development of more potent inhibitors for cancer driving mutant proteins.

### **Multivalent T-Cell Engagers for the Treatment of Prostate Cancer**

April Marple

McMaster University, Hamilton, Canada

Purpose: Immunotherapeutics, such as bispecific T-cell engagers (BiTEs), have greatly advanced targeted cancer treatments. However, BiTE efficacy remains poor against solid tumors due to systemic toxicity, short plasma half-lives and off-site targeting from their singular high-affinity cancer-targeting antibody-fragment. Here, we report a new antibody-conjugate scaffold to synthesize PEGylated. Multivalent T-cell engagers (MuTEs) with a small molecule avidity-based targeting system towards the development of bispecifics with lower rates of off-site targeting with improved systemic toxicity and plasma half-lives. These MuTEs were tested in the treatment of prostate specific membrane antigen (PSMA) positive cancer cells utilizing Glutamate-Urea-Lysine (GUL) targeting ligands. Methods: Anti-CD3 antibody clones, UCHT-1 and OKT3, were modified with

heterobifunctional short PEG linkers and GUL ligands (PEG<sub>x</sub>-GUL) at increasing linker length and GUL content. MuTEs were tested in co-cultures of T-cells and cancer cells (PSMA positive and negative) to demonstrate targeted cytotoxicity at varying effector-to-target ratios and dosages. Avidity was tested in low and high-expressing PSMA cell lines. Cytotoxicity was determined by luminescence in luciferase expressing cells. Results: Increasing the number of PEG units on the antibody significantly reduced toxicity of the antibody and the addition of GUL ligands allowed for targeted killing in PSMA positive cell lines UCHT-1 and OKT3 modified with 6-8 PEG<sub>12</sub>-GUL showed specific cytotoxicity in low and high PSMA expressing cell lines. The EC<sub>50</sub> values of UCHT-PEG<sub>12</sub>-GUL varied by a factor of ~10 (0.658 vs 0.071 nM) for LNCaP (low-expressing) and HEK293-PSMA (high-expressing), demonstrating the ability to optimize MuTEs for preferential killing of high-expressing PSMA cells with controlled dosing. Conclusion: The antibody-conjugate scaffold allows for the rapid development of PEGylated MuTEs to preferentially kill cells that highly express cell surface targets, which will help avoid off-site targeting and systemic toxicity. The PEGylated antibody scaffold can be further developed to increase plasma half-lives to improve solid tumor accumulation.

### **Stability studies of commercial corticosteroid suspensions**

Mouna Ayad,<sup>1</sup> Leen Moussa,<sup>2</sup> Johannes M Froehlich,<sup>3</sup> Simon Matoori,<sup>1</sup>

<sup>1</sup>Université de Montréal, Montreal, Canada; <sup>2</sup>Université de Montréal, Montréal, Canada; <sup>3</sup>Klusapothke Zurich, Zurich, Switzerland

Purpose: Particulate corticosteroid suspensions are widely used for epidural, transforaminal and perineural injection for lumbar pain treatment (1). The administration of these suspensions was associated with post-procedural adverse events such as neurovascular embolism, lesion in the spine, paralysis, and death in certain patients (1). These adverse events may be related to particle size differences of corticosteroid suspensions. Size may also be influenced by acidic pH (inflammation) and plasma proteins such as albumin. The aim of this study is to measure particle size of corticosteroid suspensions at different pH values and in presence of albumin. Method: Five commercial corticosteroid suspensions of triamcinolone, methyl prednisolone, and betamethasone were analyzed. The pH was adjusted to 6.0 and 7.4. Albumin was added at 50 g/L. Size measurements were performed by static light diffraction (Beckman Coulter) and presented in terms of median volume distribution (D<sub>50</sub>). Results: The median size of the corticosteroid suspensions varied from 5.8 to 11.2 mm (triamcinolone), 101 to 124 mm (methyl prednisolone), 15.3 to 20.4 mm (betamethasone). Changes in particle size were small at lower pH and in the presence of albumin except for one methyl prednisolone suspension. Conclusion: The median sizes of the investigated commercial corticosteroid suspensions differed between products but remained in the low micron range. The size of the particles at low pH and in presence of albumin was not significantly different except for one suspension. Investigations in different biorelevant fluids (e.g., serum, presence of local anesthetics and contrast agents) and of other particle properties (e.g., surface charge) are warranted to improve our understanding of stability-influencing parameters.

### **Novel Amide Derivatives as Modulators of Amyloid-Beta Aggregation**

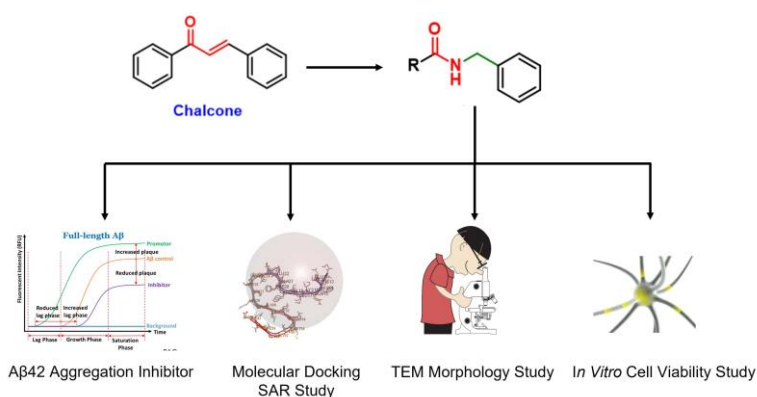
Yusheng zhao

School of Pharmacy, Faculty of Science, University of Waterloo, Waterloo, Canada

Purpose: Alzheimer's Disease (AD), the misfolding and aggregation of amyloid-beta 42 (A $\beta$ 42) is one of the hallmarks underlying its pathophysiology. Small molecule modulators that target various protein species of A $\beta$ 42 aggregation can reduce the overall burden of toxic A $\beta$ . The purpose of this study was to design, synthesize and evaluate novel amide derivatives' ability to modulate the aggregation of A $\beta$ 42 and to understand the mechanism of aggregation. Methods: The small molecule library was designed based on the structure of curcumin and chalcone. To rule out pan-assay interfering, the  $\alpha$ ,  $\beta$ -unsaturated system was replaced by amide bond and various



bioisosteres were included. The target compounds were synthesized, purified, and characterized by chromatography, NMR, LCMS, and UPLC. The modulatory activity on A $\beta$ 42 aggregation was screened by thioflavin T (ThT) based kinetic study. The morphology of aggregates was obtained by transmission electron microscopy (TEM) study. Computational modeling was used to investigate the binding interactions and to understand the structure-activity relationship. Results: The small molecule library was synthesized by coupling acid chlorides and amines in good-to-high yields (71-96%) and purity (96.1% to 99.6%) A $\beta$ 42 kinetic assay showed that nearly all compounds exhibit moderate ability to inhibit A $\beta$ 42 (5  $\mu$ M) aggregation. The inhibition rate ranges from 11-36% at 10  $\mu$ M and 41-71% at 25  $\mu$ M. TEM studies showed a significant reduction in the formation of A $\beta$ 42 in the presence of some compounds. Molecular docking study indicates that these small molecules undergo interactions with the core <sup>16</sup>KL<sup>21</sup>VFF<sup>21</sup>A region to stabilize the aggregation process. Conclusion: A library of novel amide derivatives was designed, synthesized, and characterized. The primary biological screening showed that these derivatives can moderately inhibit the A $\beta$ 42 aggregation. These studies demonstrate that this class of compounds is capable of binding to A $\beta$ 42 and preventing their aggregation. The results suggest their application to study the mechanisms of aggregation and to design novel therapeutic agents.



## In-vitro Model to Forecast the Lymphatic Uptake/Inhibition of Drugs via Chylomicrons

Malaz Yousef,<sup>1</sup> Nadia Bou Chacra,<sup>2</sup> Neal Davies,<sup>1</sup> Raimar Loebenberg,<sup>1</sup>

<sup>1</sup>Faculty of Pharmacy and Pharmaceutical Sciences, University of Alberta, Edmonton, Canada; <sup>2</sup>University of Sao Paulo, Sao Paulo, Brazil

**Purpose.** Lymphatic uptake of drugs through chylomicrons (lymph-carried species produced by intestinal cells) imparts important pharmacokinetic and pharmacodynamics implications. However, the biophysics of in-vitro systems and prediction of in-vivo lymphatic disposition has not been mechanistically examined.<sup>1,2</sup> The aim of this study was to investigate the oral lymphatic uptake of drugs and their inhibition via a novel in-vitro model. **Methods.** The intestinal lymphatic system was mimicked in-vitro using Franz cells and intralipid (an emulsion resembling chylomicrons). Solutions of model lymphotropic drugs (rifampicin, cannabidiol, and quercetin) were added to the donor compartment at different concentrations (0.5-2 mg/ml). The receiver compartment was maintained at 37.0 $\pm$ 0.5  $^{\circ}$ C and magnetically stirred at 600 rpm. It was filled with either intralipid or intralipid containing pluronic L-81 (1%-15%) or chloroquine (5%). Octanol-immersed 0.22  $\mu$ m Polyvinylidene Fluoride (PVDF) membranes were used to separate the compartments. At different intervals, 0.2 ml samples were taken and extracted with organic solvents (extraction efficiency >92%) before HPLC analysis to determine the rate and extent of uptake over time. **Results.** The cumulative percentages of the different drugs of the same concentration (1 mg/ml) in the receiver compartment were found to be as follows: 12.05%, 33.29%, and 36.12% for rifampicin, cannabidiol, and quercetin, respectively. The receiver compartment contained 0% of the rifampicin when 15%, 10%, and 1% of the pluronic were used and nearly 50% of what was reported before with 0.1% pluronic.



Moreover, chloroquine significantly affected the release of both rifampicin and quercetin (1% or less was released) into the receiver compartment. Conclusion. The new model showed promising results that can potentially be used to study and may predict the intestinal lymphatic uptake via chylomicrons with various excipients and drugs that can inhibit the process by influencing chylomicron integrity. In-vitro models can mechanistically demonstrate chylomicrons' uptake of drugs and inhibition of this process.

### **Development and characterization of emulsion-based immunoadjuvant nanovaccines**

Ramin Mohammadi,<sup>1</sup> Pooja Choudhary,<sup>2</sup> Heather L Wilson,<sup>2</sup> Azita Haddadi,<sup>1</sup>

<sup>1</sup>Division of Pharmacy, College of Pharmacy & Nutrition, University of Saskatchewan, Saskatoon, SK S7N 5E5, Canada, Saskatoon, Canada; <sup>2</sup>Vaccine and Infectious Disease Organization (VIDO), University of Saskatchewan, 120 Veterinary Road, Saskatoon, Saskatchewan S7N5E3, Canada, Saskatoon, Canada

**Purpose:** The main goal of this project is to investigate strategies for development of vaccine nanoparticles co-encapsulating ovalbumin as a model antigen and emulsion based immunoadjuvants. An oil in water emulsion, squalene, and a water in oil emulsion, Montanide 61, will be used in this study to enhance the immunoadjuvant efficiency of the emulsions. **Method:** Poly (lactide-co-glycolide) (PLGA) nanoparticles were prepared based on solvent evaporation and ultrasonication techniques. Various formulations of nanoparticles were developed carrying protein and immunoadjuvants, and then characterized with respect to their particle size, zeta potential, and polydispersity index using the ZetaSizer instrument through dynamic light scattering technique. Different formulations parameters such as polymer concentration, volume, ultrasonication speed and time, antigen dose and immunoadjuvant dose were investigated to optimize the nanoparticulate vaccines. **Results:** Many experiments and optimization steps were conducted to achieve optimum nanovaccines loaded with the immunoadjuvants and to evaluate their physicochemical properties. The data obtained for the size of our nanoparticles are shown to be in the range of 200-300 nm and their zeta potential is between -20 mv and -30 mv. Yield of the production technique was also optimized. **Conclusion:** These novel nanovaccines are developed in a suitable range for effective immune cell uptake. Our target is to improve the delivery of emulsion based adjuvants and minimize their dose to avoid their side effects.

### **In vitro study of a foamable microemulsion for improved topical delivery of diclofenac sodium**

Braa Hajjar,<sup>1</sup> Jieyu Zuo,<sup>1</sup> Chulhun Park,<sup>1</sup> Shirzad Arzarmi,<sup>1</sup> Daniela Amaral Silva,<sup>1</sup> Nadia Bou Chacra,<sup>2</sup> Raimar Loebenberg,<sup>1</sup>

<sup>1</sup>Faculty of Pharmacy and Pharmaceutical Sciences, University of Alberta, Edmonton, Canada; <sup>2</sup>University of Sao Paulo, Sao Paulo, Brazil

**Purpose:** Topical microemulsions (ME) are a novel and advanced topical delivery system that can enhance drug solubility and permeability across the skin. Foams have excellent patient compliance due to their ease of administration and the convenience of application. This study investigated a foamable microemulsion as an alternative topical dosage form for diclofenac sodium (DS). **Method:** The physicochemical properties (optical clarity, percentage transmittance, homogeneity, consistency of formulation, globule size, zeta potential, pH, conductivity, viscosity, and morphology) of the microemulsion with and without DS were investigated. The foam quality and foam stability with and without DS were determined over 90 days. Franz diffusion cells were used to assess the in vitro drug release from a DS-loaded foam and compared with a commercial topical product. **Results:** A foamable and 90 days stable DS-loaded ME was successfully formulated by evaluating the transparency and translucency, globule size, zeta potential, and foam quality. The foam exhibited an increased rate and extent of drug release compared to the commercial product. **Conclusion:** The foamable DS-loaded ME was stable for three months. The tested formulation has great potential to enhance the topical delivery of DS for pain management

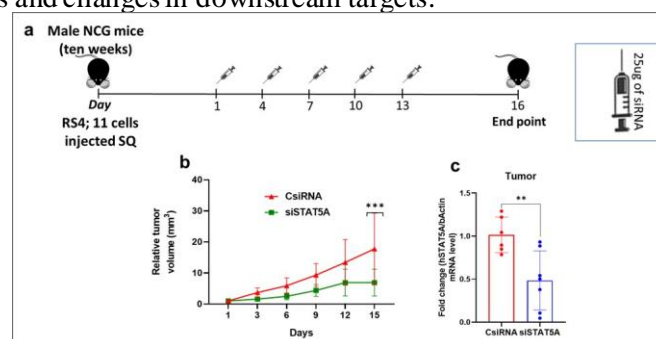
locally. Foamable ME is a promising alternative to the current topical formulation of DS. Funding: This study is supported by Taibah University (Saudi Arabia), Alberta Innovates Graduate Student Scholarship (Canada), and Mitacs Accelerate (IT13686, Canada).

### Lipid-substituted polyethylenimine conjugate mediated STAT5A siRNA reduces the growth of acute lymphoblastic leukemia in vivo

Mohammad Nasrullah, Luis C Morales, Remant KC, Hasan Uludag

University of Alberta, Edmonton, Canada

**Purpose:** Acute Lymphoblastic Leukemia (ALL) is the most common cancer in children and teens. It originates from immature forms of lymphocytes. Poor response to existing therapy and high rates of relapse in ALL, raised the need to develop alternative therapies. Recently, we reported that lipid-substituted low molecular weight polyethylenimine PEI (PEI-Lipid) complexed STAT5A siRNA (siSTAT5A) downregulates STAT5A and inhibits ALL cell growth in vitro.<sup>1</sup> Our current study is aimed to investigate the efficiency of PEI-Lipid to deliver STAT5A siRNA in the mouse model and to assess the in vivo potential of tumor growth inhibition. **Method:** We prepared the PEI-Lipid, as described previously.<sup>1</sup> Acute lymphoblastic RS4;11 cells were injected subcutaneously (SQ) into triple immunodeficient (NCG) male mice to develop the human xenograft model. The tumor volume was measured every 3 days and subjects were recruited for the study when the tumor size reached >100 mm<sup>3</sup>. Five doses of 25µg of siSTAT5A complexed with PEI-Lipid were injected SQ every 3 days. After 3 days of the final dose, tumors were harvested for RT-qPCR analysis to evaluate the STAT5A expression. Scrambled control siRNA (CsiRNA) was used as the negative control. **Results:** SQ treatment of the CsiRNA group resulted in significantly higher growth (p=0.0005) of xenografted ALL tumors compared to the siSTAT5A group. Furthermore, human STAT5A expression level was measured in tumor samples and found to be significantly downregulated (p=0.0073) in the siSTAT5A group compared to the CsiRNA group. **Conclusion:** Significant downregulation of STAT5A expression in xenografted tumor samples in response to PEI-Lipid complexed siSTAT5A causes reduced tumor volume in an ALL-xenograft mouse model. This PEI-Lipid can be used as an effective non-viral carrier to deliver RNA therapeutics into in vivo models. More studies are required to evaluate the immune response levels and changes in downstream targets.



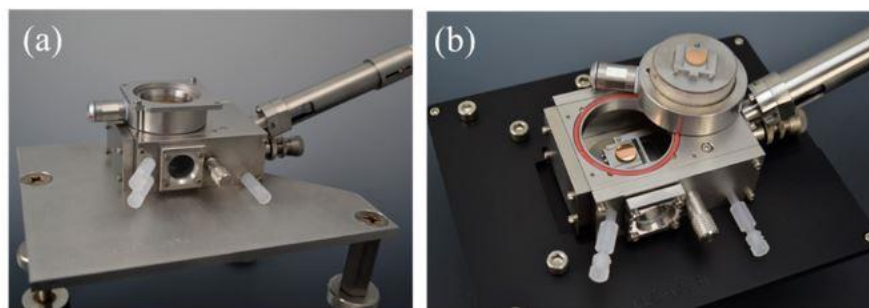
### Tuning surface-surface interaction by using a non-invasive method

Nahid Hassanpour,<sup>1</sup> Daria Camila Boffito,<sup>2</sup> Xavier Banquy,<sup>1</sup>

<sup>1</sup>Universite de Montreal, Montreal, Canada; <sup>2</sup>Polytechnique, Montreal, Canada

Tuning surface-surface interaction by using a non-invasive method Nahid Hassanpour<sup>1</sup>, Daria Camila Boffito<sup>2</sup>, Xavier Banquy<sup>1</sup> <sup>1</sup>Faculty of Pharmacy, Université de Montréal, Montréal, QC H3C 3J7, Canada <sup>2</sup> Department of Chemical Engineering, Polytechnique Montréal, Montréal, H3C 3A7 Qc, Canada

Understanding the surface-surface cell interactions or cell interaction with the extracellular environment such as cell-proteins interactions is a major factor to know the function of living organs. Controlling the underlying mechanism of cell-surface interactions at interfaces is one of the most demanding aims for scientific fields and applications in diagnostic microarrays, biosensing, drug delivery, and regenerative medicine [1,2]. Within the last few years, many methods have been developed to manipulate and diminish cell attachment or detachment such as Ultrasound (US). For decades US used it in medical diagnosis and imaging [3], enhancing the efficacy of many treatments and drug delivery [4] even tribology [5]. But knowing the effect of US on surface interactions (adhesion, lubrication) is poorly investigated. Such knowledge could help understand how living tissue interacts with biomaterials and how the US could help modulate such interactions. Our hypothesis is that a controlled amount of ultrasound radiation will manipulate the surface-surface interactions from the adhesive (which is essential for capture) to repulsive (which facilitates evasion and penetration). The experiments will be performed using the surface forces apparatus (SFA) which allows to quantitatively measure interaction forces between two surfaces in the presence of external stimuli such as US to evaluate the impact of ultrasounds on the interaction forces between surfaces to identify the key parameters that can eliminate any possible adhesion. Our results showed that controlled amounts of ultrasound radiations, including amplitude and frequency as tuning parameters, modulate surface-surface interactions. Specifically, we observed that ultrasound radiation transfers the state of surface-surface interaction from adhesive to repulsive, a promising result for the application of ultrasound in modulating cell-cell membrane interactions.



### Heat-triggered delivery of synergistic chemotherapies in murine models of breast cancer

Xuehan Wang, Michael Dunne, Maximilian Regenold, Christine Allen

Leslie Dan Faculty of Pharmacy, University of Toronto, Toronto, Canada

**Purpose:** Doxorubicin (DOX) is among the most commonly used chemotherapy drugs, including in the treatment of breast cancer.<sup>1</sup> However, its use is limited due to cardiotoxicity.<sup>2</sup> Several approaches have been developed to mitigate the off-target effects of DOX. Among these is a thermosensitive liposomal formulation of DOX (i.e., ThermoDox®) that has previously been evaluated in Phase III clinical trials. Despite the improvements in drug delivery to the tumor site afforded by this approach, a significant amount of free DOX can enter the systemic circulation potentially contributing to the observed normal tissue toxicity.<sup>3</sup> To reduce DOX doses and prevent adverse effects, our lab previously identified a highly synergistic drug combination of DOX with the heat shock protein 90 inhibitor alvespimycin (ALV). This combination has been previously developed into a heat-triggered drug delivery approach.<sup>4</sup> Here we investigate this drug combination together with localized mild hyperthermia (HT) in the treatment of both immunocompromised and immunocompetent breast cancer models. **Methods:** SCID mice bearing MDA-MB-231 breast cancer xenografts and BALB/c mice with orthotopic 4T1 breast cancer were treated with either in-house manufactured ThermoDox at different doses (i.e., 3 or 5 mg/kg), ThermoDox and ThermoALV combination (i.e., 3 and 15 mg/kg respectively), all in combination with mild HT, or with saline once per week for three weeks. Tumor volumes and animal weights were monitored to determine treatment

efficacy and toxicity. Results: The combination treatment was able to reduce toxicity (ie, less bodyweight loss) while simultaneously prolonging median survival times compared to the high dose ThermoDox treatment in the MDA-MB-231 model. Similar trends were observed in the immunocompetent 4T1 model. Conclusion: Triggered-drug delivery of DOX and ALV at a synergistic ratio is able to achieve similar treatment efficacy while lowering the DOX dose by 40%. This strategy proves to be a powerful approach to address the inherent toxicity of doxorubicin.

### **Triggered Release of Vinorelbine from Thermosensitive Liposomes**

Maximilian Regenold, Kan Kaneko,<sup>2</sup> Xuehan Wang, Christine Allen

Leslie Dan Faculty of Pharmacy, University of Toronto, Toronto, Canada

Purpose: Nanomedicines can enable targeted drug delivery to the tumor site. This targeted treatment approach has enormous potential to mitigate many of the side effects associated with long-term systemic exposure to chemotherapeutics. This is particularly important in childhood cancer patients who often develop treatment related adverse effects later in life. However, several challenges such as limited drug release and heterogeneous drug distribution at the target site, have prohibited the widespread success of these strategies. Heat-triggered drug delivery via thermosensitive liposomes has been proposed as an approach to address these challenges. Our lab has previously developed a thermosensitive liposome formulation of the commonly used vinca-alkaloid vinorelbine (ThermoVRL) [1]. Here we demonstrate that this triggered drug delivery approach has the potential to repurpose this conventional chemotherapy drug by conferring improved targetability. Methods: Subcutaneous Rh30 tumors in female SCID mice were treated iv with either free VRL, a non-thermosensitive liposomal formulation of VRL (NTSL-VRL), or with ThermoVRL at 15 mg/kg. All treatments were administered in combination with mild hyperthermic heating localized to the tumor (42.5 °C for 25 min). Animals were sacrificed at various time points and VRL levels in whole blood, tissues, and tumors was measured via HPLC-MS. Results: Liposomal encapsulation significantly increased the amount of VRL delivered to the tumor compared to the administration of free drug. More importantly, VRL administered as ThermoVRL was able to improve the tumor specific drug uptake. Specifically, when administered as ThermoVRL, VRL partitioning into tumor tissue was increased nearly two-fold compared to other organs. When administered as free VRL or NTSL-VRL no such improvements were noted. Conclusion: Triggered-drug release of VRL from ThermoVRL offers a targeted delivery approach that increases the amount of bioavailable drug delivered specifically to the tumor compared to the administration of free drug or non-thermosensitive, traditional liposomes.

### **Extraction, Isolation and Characterization of Novel Active Constituents from a Medicinal Plant Source**

Anoushka Tyagi,<sup>1</sup> Arash Shakeri,<sup>2</sup> Yusheng Zhao,<sup>2</sup> Praveen Nekkar Rao,<sup>2</sup> Okechukwu Igboeli,<sup>3</sup>

<sup>1</sup>Science and Business Program, Faculty of Science, 200 University Ave West, University of Waterloo, Waterloo, Canada; <sup>2</sup>School of Pharmacy, Health Sciences Campus, 200 University Ave West, University of Waterloo, Waterloo, Canada; <sup>3</sup>Department of Biology, Faculty of Science, 200 University Ave West, University of Waterloo, Waterloo, Canada

Purpose: There are limited therapeutics for Alzheimer's disease (AD), a progressive neurodegenerative disease. We aimed to isolate and characterize novel active ingredients from a medicinal plant to identify potential therapeutics for treating AD. Methods: The plant material was extracted using methanol followed by ethyl acetate and hexane/ACN-H<sub>2</sub>O washes to remove salts and lipids, respectively ACN-H<sub>2</sub>O fraction was subjected to flash chromatography using the C18 reversed-phase column. This yielded 13 fractions which were subjected to antioxidant assay using the stable free radical 2, 2-diphenyl-β-picrylhydrazyl (DPPH) at 0.1, 1, 5, 10, 50, and 100 µg/ml and anti-amyloid-beta (Aβ) assay at 1, 5, 10, and 25 µg/ml using the thioflavin T (ThT) based fluorescence

aggregation kinetics study. Results: The solvent systems and separation methods were optimized using several analytical methods including flash chromatography, LCMS and  $^1\text{H}/^{13}\text{C}$  NMR to isolate and characterize fractions from the plant material. In the antioxidant assay, fractions F2 and F3 exhibited ~49% scavenging activity at 50  $\mu\text{g}/\text{ml}$  and were not as potent as the reference agents resveratrol and trolox (90% and 96% scavenging activity). In the anti- $\text{A}\beta$  assay, fraction F2 exhibited excellent inhibition at 10 and 25  $\mu\text{g}/\text{ml}$  (90% and 95% inhibition respectively) and was much more potent compared to the reference agent resveratrol (82% and 92% inhibition at 10 and 25  $\mu\text{g}/\text{ml}$  respectively). Conclusion: Our studies demonstrate that novel active constituents from a proprietary plant source exhibit antioxidant and anti- $\text{A}\beta$  activity. Few isolated fractions exhibited excellent antioxidant properties in the DPPH assay and also demonstrated anti- $\text{A}\beta$  activity in the in vitro ThT assay suggesting their potential as novel therapeutics. Future studies will be carried out to complete the structural elucidation and consider potential synthetic strategies to obtain novel active ingredients for further biological evaluation.

### **Comparing the in vitro performance of cross-linked to conventional polyester microparticles**

Jack Bufton, Pauric Bannigan, Christine Allen

University of Toronto, Toronto, Canada

Purpose: Polymeric microparticles can be engineered to provide sustained and/or localized drug release profiles. The polyester poly(lactide-co-glycolide) (PLGA) makes up almost all FDA-approved microparticles. By design, PLGA is prone to degradation and hydrolysis in aqueous environments. This results in a weakening of the polymeric matrix, increases in drug release rates, and a shortening of total drug release duration. In this work, PLGA microparticles (MP) and cross-linked poly(lactide-co-allyl-glycolide) (PLAGA) microparticles (xMP) were prepared using an in-house microfluidic droplet generation platform. The size, drug loading, in vitro release, and structural integrity (in aqueous media) of the microparticles were compared. Methods: MP was manufactured using PLGA (Resomer® 504H, MilliporeSigma) and loaded with celecoxib (CXB) Reactive droplets of PLAGA (AI108, PolySciTech®) were exposed to UV light to prepare xMP, and CXB was loaded post-production using a swelling equilibrium method. In vitro release was evaluated for each system using a sample-and-separate method. Light microscopy was used to assess the integrity of non-loaded microparticles following exposure to release media (PBS and ionic surfactant). Results: The drug loading level for MP and xMP was  $16\pm 0.5\text{wt}\%$  and  $23\pm 0.5\text{wt}\%$  (encapsulation efficiency of  $82\pm 3\%$  and  $60\pm 1\%$ , respectively). After 16 days, MP and xMP showed ~95% and ~25% fractional drug release in vitro (Fig 1a). The average diameters of the non-loaded xMP and MP were  $68\pm 4$  and  $42\pm 20$   $\mu\text{m}$ . Following 16 days in release media, the average diameter of non-loaded xMP and MP increased by <2% and 113%, respectively (Fig 1b). Conclusions: Cross-linked xMP has potential to afford slower and more sustained drug release in vitro. Cross-linking of the polymer backbone may prevent swelling and chain hydrolysis, phenomena that are known to increase drug release rates. The use of cross-linked PLAGA across various drug delivery systems may result in more sustained release profiles.

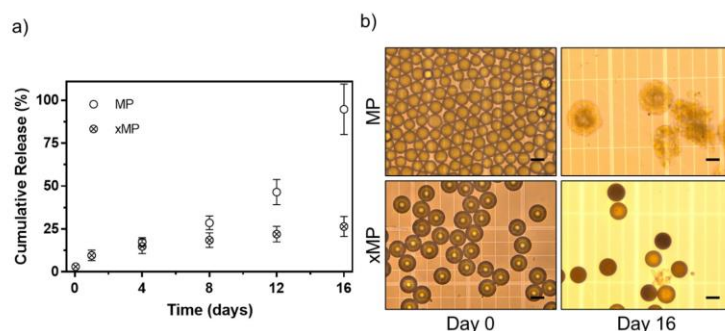


**Figure 1.** Average fractional cumulative *in vitro* release of non-crosslinked (MP) and cross-linked (xMP) microparticles loaded with celecoxib  $\pm \sigma$  (n=3) (a). Representative light microscopy images of non-loaded MP and xMP microparticles at 0 and 16 days under *in vitro* release conditions (b). The scale bars represent 50  $\mu\text{m}$ .

## Computational Insight into the Molecular Interactions between the TIR Domain of TLR4 and its Antagonists

Ismat Luna

University of Alberta, Edmonton, Canada

**Purpose:** Recent biochemical studies done by Babolmorad et al have identified the association of cisplatin with TLR4 activation.<sup>1</sup> They demonstrated that TLR4 plays a critical role in mediating cisplatin-induced ototoxicity (CIO) response *in vitro* which can be inhibited by small-molecule TAK-242. However, the precise mode of action by which TAK-242 inhibits TLR4 signaling after binding to the receptor has remained uncertain. The purpose of this project is to computationally investigate the molecular interaction of TAK-242 and some of its synthetic analogs with TLR4 for inhibiting its downstream signal transduction. **Methods:** As TAK-242 is known to bind in the TIR domain of TLR4,<sup>2</sup> we used the three-dimensional model of this domain in dimer forms to conduct our *in silico* studies. The dimeric TIR domain was subjected to molecular dynamic (MD) simulation in an explicit solvent environment and subsequent clustering analysis to extract the dominant protein conformations. The obtained dominant conformations were then used in molecular docking studies with some selected inhibitors. The subsequent MD simulations of protein-ligand complexes were performed to characterize the structural changes introduced by small molecule inhibitors binding to TLR4 compared to free TLR4 form. **Results:** Root-mean-square deviation (RMSD) and atomic fluctuations data showed a clear difference between the bound and free states for the stability and dynamicity of the TLR4 receptor. Binding affinities calculated over the simulations allowed us to obtain a relative rank between compounds which was fairly consistent with the experimental data about the activities. The results from the MMGBSA calculations showed a notable difference in binding energies between strong and weak antagonists. These data highlighted a direct correlation between binding energy and antagonist activity. **Conclusions:** In conclusion, our work disclosed the dynamical and structural perspectives to explain the molecular interactions between TLR4 receptor and its small molecule inhibitors, leading to further optimization of new derivatives.

## Repurposing Pyronaridine as a novel inhibitor of heterodimeric ERCC1-XPF DNA endonuclease complex for targeted sensitization of colorectal cancer to platinum-based chemotherapeutics

Parnian Mehinrad,<sup>1</sup> James Donnelly,<sup>2</sup> Sams M A Sadat,<sup>1</sup> David Jay,<sup>3</sup> Feridoun Karimi-Busheri,<sup>3</sup> Frederick G West,<sup>2</sup> Michael Weinfeld,<sup>3</sup> Afsaneh Lavasanifar<sup>1</sup>

<sup>1</sup>Faculty of Pharmacy and Pharmaceutical Sciences, University of Alberta, Edmonton, AB, Canada, Edmonton, Canada; <sup>2</sup>Faculty of Science, Department of Chemistry, University of Alberta, Edmonton, Canada

<sup>3</sup>Department of Experimental Oncology, Cross Cancer Institute, Edmonton, AB, Canada, Edmonton, Canada;

**Purpose:** The overall objective of this proposal is to improve the therapeutic outcome in colorectal cancer patients, especially those with locally advanced disease stages. This objective will be pursued through the repurposing of a clinically used antimalaria drug, ie, pyronaridine, as a novel inhibitor of a DNA repair enzyme, ERCC1/XPF. Inhibition of ERCC1/XPF, a heterodimeric enzyme complex with endonuclease activity that participates in the repair of DNA inter- and intra-strand crosslinks, is expected to make cells sensitive to DNA damage by platinum-based chemotherapeutics. We have developed a liposomal formulation of pyronaridine to make the chemo-sensitizing activity of the ERCC1/XPF inhibitor tumor-specific. **Methods:** A liposomal delivery system of pyronaridine was developed consisting of three phospholipids (DSPC, DSPE-PEG, Cholesterol) and a pH gradient system. Prepared formulations were characterized for their average diameter, encapsulation, and in vitro release. The cytotoxic activity of free and loaded pyronaridine in combination with Carboplatin and Oxaliplatin was assessed against HCT116 and SW620 cell lines using the MTT assay. The possibility of a synergistic effect between Pyronaridine and Carboplatin/Oxaliplatin in HCT116 was tested using the Combobenefit format. **Results:** The liposomal formulation was shown to have 99% encapsulation efficiency for the added pyronaridine. The average diameter of the liposomes was  $82.32 \pm 0.33$  nm with a polydispersity index of  $0.181 \pm 0.008$ . In media consisting of PBS and BSA, only ~50% of the loaded drug was released within 72 h. The results of the cytotoxicity study showed a significant reduction (when compared to carboplatin alone) in the viability of the HCT116 cell line following co-treatment of 0.5 mM pyronaridine (as free and particularly liposomal formulation) with carboplatin (25-100mM). Synergistic activities upon co-treatment with pyronaridine and carboplatin/oxaliplatin were observed in the concentration range of 0.075-0.3 mM pyronaridine and 4.7-9.7mM carboplatin. **Conclusion:** The preliminary results indicate a potential for pyronaridine and its liposomal formulation in chemo-sensitization of CRC to platinum chemotherapeutics.

## PHARMACOKINETICS AND PHARMACODYNAMICS

### **Effect of doxorubicin, diltiazem or losartan on metabolism and catabolism of guanosine 5'-triphosphate in red blood cell in rats**

Pollen Yeung, Sheyda Mohammadzadeh, Kelsey Mann, Remigius U Agu

Dalhousie University, Halifax, Canada

**Purpose:** Previous studies have shown doxorubicin (DOX) increased breakdown of GTP more so that ATP in red blood cells (RBC) which could be a potential surrogate biomarker for serious cardiovascular toxicity. In this study we compared the effect of doxorubicin (DOX), diltiazem (DTZ) and losartan (LOS) on GTP metabolism in RBC using a freely moving rat model. **Method:** Sprague Dawley (SD) rats ( $n = 5 - 11$ ) were each given either 10 mg/kg of DOX or DTZ, 5mg/kg of LOS or normal saline by subcutaneous injection 2 times a day for 4 doses. Blood samples were collected just before the last injection (T0) and also at 0.08, 0.25, and 1 hour after the last dose for measuring RBC concentrations of GTP and GDP. The average RBC concentrations of GTP, GDP and their ratios were compared and difference assessed by ANOVA followed by Tukey's and considered significant at  $p < 0.05$ . **Results:** RBC concentrations of GDP and breakdown of GTP to GDP in the RBC were significantly higher in the DOX treated rats compared to the other groups ( $p < 0.05$ ). Rats treated with DTZ or LOS had significantly greater metabolism of GTP from GDP in the RBC compared to the DOX treated rats ( $p < 0.05$ ). There was no difference in GTP metabolism between the DTZ and LOS treated rats ( $p > 0.05$ ). **Conclusion:** DOX (10 mg/kg) increased breakdown of GTP to GDP in the RBC DTZ (10 mg/kg) or LOS (5 mg/kg) increased metabolism of GTP in the RBC suggesting that these cardiovascular agents may have potential to alleviate cardiotoxicity induced by DOX. Further studies are needed to substantiate the finding (supported in part by funding from Dalhousie Faculty of Health and Pharmacy Endowment Foundation).

## **Down-regulation of cytochrome P450 1A1 (CYP1A1) by arsenic trioxide (ATO) in human hepatoma (HepG2) cells**

Mahmoud Elghiaty, Ayman El-Kadi

Faculty of Pharmacy and Pharmaceutical Sciences, University of Alberta, Edmonton, Canada

**Purpose:** Arsenic is a ubiquitous occupational and environmental contaminant that imposes threat to humans, however, some arsenicals are exploited for remedial purposes. Arsenic trioxide (ATO) has emerged as a successful therapy for acute promyelocytic leukemia (APL) and probably for solid tumors in the future. Both inorganic arsenic and its methylated metabolites have been shown to modulate aryl hydrocarbon receptor (AhR)-regulated xenobiotics-metabolizing enzymes including cytochrome P450 1A1 (CYP1A1), thus modifying activation/detoxification of drugs/procarcinogens. Therefore, this study aimed to investigate the possible effects of ATO on CYP1A1 in absence or presence of the archetypal AhR ligand, 2,3,7,8-tetrachlorodibenzo-p-dioxin (TCDD) using human hepatoma (HepG2) cells. **Methods:** HepG2 cells were treated with ATO (1, 5 and 10  $\mu$ M) in the absence or presence of 1 nM TCDD and/or 5  $\mu$ M Tin<sup>IV</sup> mesoporphyrin<sup>IX</sup> (SnMP) CYP1A1 and heme oxygenase 1 (HMOX1) expression was evaluated at mRNA and protein levels using qPCR and western blotting, respectively. EROD assay assessed CYP1A1 activity Luciferase assay was conducted in HepG2 cells transfected with xenobiotic response element (XRE)-luciferase reporter plasmid. **Results:** ATO showed significant concentration-dependent inhibition of TCDD-mediated induction of CYP1A1 mRNA, protein, and activity, with significant induction of HMOX1 mRNA and protein. Additionally, ATO inhibited luciferase activity elicited constitutively and inducibly by TCDD. Also, inhibition of HMOX1 by SnMP partially restored ATO reduction of TCDD-mediated EROD activity **Conclusion:** Our findings show that ATO down-regulates CYP1A1 expression at mRNA, protein, and catalytic activity. The alteration of CYP1A1 is mediated by transcriptional and post-translational mechanisms. These findings imply possible involvement of ATO in pharmacokinetic interactions with the substrates of CYP1A1. This work was supported by the Natural Sciences and Engineering Research Council of Canada (NSERC) Discovery Grant [RGPIN 250139] to AOSE. MAE is a recipient of the Rachel Mandel Scholarship in Lymphoma and Other Blood Cancers and the Alberta Innovates Graduate Student Scholarship.

## **Investigating murine sex and strain differences in kidney microsomal and cytosolic scaling factors**

Michael Doerksen,<sup>1</sup> Robert Jones,<sup>2</sup> Michael WH Coughtrie,<sup>1</sup> Abby Collier,<sup>1</sup>

<sup>1</sup>The University of British Columbia, Vancouver, Canada; <sup>2</sup>Genentech Inc, South San Francisco, United States

**Purpose.** The kidney, in addition to maintaining fluid and electrolyte homeostasis, is an important extrahepatic organ involved in xenobiotic metabolism. The scaling factors microsomal protein per gram of kidney (MPPGK) and cytosolic protein per gram of kidney (CPPGK) can be used for in vitro-in vivo extrapolation of renal metabolism data. These can be incorporated into pharmacokinetic models to understand drug disposition and for clinical trial dose selection. The objective of this research is to investigate murine strain (CD-1 and C57BL/6) and sex differences in scalars by parameterization of scaling factors and evaluation of microsomal intactness. **Methods.** Whole kidneys (n=5 per strain and sex) were dissected and homogenized in either a sucrose-HEPES or Tris-HCl buffer condition. Following differential centrifugation (10,000x g, then 100,000x g), to generate microsomal and cytosolic fractions, protein content was quantified, scalars parameterized, and intactness of microsomes assessed with mannose-6-phosphatase assay. **Results** Preliminary data suggests no strain and sex differences for CPPGK in either buffer condition MPPGK scalars were significantly different between female CD-1 and male C57BL/6 mice in the sucrose-HEPES buffer (10.9  $\pm$  1.3 vs 13.5  $\pm$  0.6 mg protein/g kidney) and Tris-HCl (9.3  $\pm$  1.2 vs 13.0  $\pm$  2.0 mg protein/g kidney) buffer, but differences were not observed between other



strains and sexes There were no significant differences in microsomal intactness for the Tris-HCl buffer condition, however intactness was significantly lower for male C57BL/6 ( $63.2 \pm 1.7\%$ ) compared to female CD-1 ( $73.2 \pm 4.7\%$ ) and male CD-1 ( $74.5 \pm 3.9\%$ ) sucrose-HEPES derived microsomes. Conclusion. These data suggest potential sex and strain differences in renal microsomal scaling factors and intactness. Additionally, differences in trends observed between sucrose-HEPES and Tris-HCl buffer conditions for microsomal intactness highlights the importance of methodological considerations for scalar parameterization. Further investigations will parameterize these scaling factors and investigate intactness in Swiss Webster kidneys.

### **Pharmacokinetics of cycloheximide in rats and evaluation of its effect as a blocker of intestinal lymph absorption**

Hamdah Al Nebaihi, Neal Davies, Dion Brocks

Faculty of Pharmacy and Pharmaceutical Sciences, University of Alberta, Edmonton, AB, Canada, Edmonton, Canada

**Purpose:** cycloheximide (CHX) is a protein synthesis inhibitor that can block the formation of intestinal lymph. It has been used as a non-surgical tool to study the contribution of intestinal lymph in drug absorption. Although, CHX has been shown to inhibit intestinal flow, the doses used were arbitrary and exposures with these doses were not studied. Moreover, the dose levels used (3 mg/kg) are associated with significant toxicity and administered via intraperitoneal (ip) route, which may bypass the enterocytes where the compound acts. The aim of this study is to understand the pharmacokinetics (PK) and effect of CHX at reducing fat absorption. **Methods:** Jugular-vein cannulated (JVC) male Sprague-Dawley rats were administered 0.5 mg/kg CHX by oral (po), ip, and intravenous (iv) route. Serial post-dose blood samples were drawn for 24 h and assayed using a published LC-MS/MS method.<sup>(1)</sup> Another four JVC rats were given, peanut oil (2 mL/kg) on day 1, and on day 2, peanut oil 30 min after 25 mg/kg CHX po. Blood samples were measured for CHX, cholesterol and triglyceride after the gavages. **Results:** The oral absolute bioavailability (F) of CHX was 47%. The relative bioavailability after ip doses was higher than after iv doses, suggesting a process such as enterohepatic recycling. The relative F of CHX after po doses compared to ip was 15%. Significant reductions in the area under curve (AUC) of serum lipids were seen after oral CHX as expected with inhibition of intestinal lymph flow; the reduction was 51% and 23% in cholesterol and triglyceride AUC, respectively. **Conclusion:** This study is the first to report the pharmacokinetics of cycloheximide in rats, and showed that after oral doses it was able to reduce lipid absorption and presumably chylomicron formation.

### **Use of Bayesian forecasting to estimate the pharmacokinetic parameters of ropivacaine in the rat**

Shamima Parvin, Dion Brocks

Faculty of Pharmacy and Pharmaceutical Science, University of Alberta, Edmonton, Alberta, Canada, Edmonton, Canada

**Purpose:** Bayesian forecasting can be used to estimate pharmacokinetic parameters (PKP) using sparse blood sampling. It is used clinically to find PKP in patients given drugs requiring concentration monitoring. Here we sought to explore its utility in rats given ropivacaine for which there were only a small number of plasma concentrations available. **Methods:** To use the method, population estimates of mean and standard deviation are required. Estimates of ropivacaine clearance (CL/F) volume of distribution (Vd) and speed of absorption such as tmax were found (Drug Delivery, 2011; 18(5):361). Webplotdigitizer was used to determine the PK profile after subcutaneous doses of 10 mg to 200 g. Sprague Dawley rats The profile best fit to a one compartment model. Three jugular vein-cannulated Sprague Dawley rats were given subcutaneous doses of 7.5 to 15 mg/kg on each of two days 6 days apart. After each dose, two blood samples were obtained 0.5 to 6 h postdose. Plasma was assayed using HPLC-UV. Plasma concentrations were input into a Microsoft Excel add in (PKB-est) along with the literature PKP, an estimate of assay precision drug doses. **Results:** The mean CL/F, Vd/F and tmax from the

literature were  $4.37 \pm 0.65$  L/h/kg,  $11.4 \pm 3.3$  L/kg and  $1.70 \pm 0.22$  h, respectively. Using the Bayesian method and rat concentrations, the estimates were  $785 \pm 27$ ,  $114 \pm 34$  L/kg and  $091 \pm 016$  h, respectively. The Bayesian method appeared to yield higher CL/F but similar Vd/F as the literature report. However, the weights (428 g) of our rats were higher than in the published study (200 g). This could reflect an age-related difference in metabolism. Indeed, it was reported that CYP3A in rat is higher in 400 g than 200 g Sprague-Dawley rats. Conclusion: Using sparse sampling the Bayesian method appeared to provide reasonable estimates of the PKP of ropivacaine in the Sprague-Dawley rat.

### **Intracellular Disposition of the CD36 Scavenger Receptor**

Catherine Le<sup>1</sup>, Mukandila<sup>1</sup> Mulumba, Sylvie Marleau<sup>1</sup>, Huy Ong<sup>1</sup>, William Lubell<sup>2</sup>

<sup>1</sup>Faculty of Pharmacy and <sup>2</sup>Department of Chemistry, University of Montreal, Montreal, Canada

**Purpose:** The CD36/SR-B2 scavenger receptor, expressed by macrophages, is one of the main receptors involved in the internalization and metabolism of oxidized low-density lipoproteins in atherosclerosis development. We undertook studies to delineate the endocytic route of the CD36 receptor complex following its binding to a synthetic CD36 ligand Cyclic azapeptide derivatives of GHRP-6 (His-D-Trp-Ala-TRP-D-Phe-Lys-NH<sub>2</sub>) were developed and the prototype MPE-298 featuring high potency and selectivity binding towards the CD36 receptor was used. We hypothesize that MPE-298 promotes the internalization of the CD36 receptor-azapeptide complex through the endosomal and recycling pathway. **Methods:** J774 macrophages, transfected with an mCD36-GFP, were incubated with 100 nM MPE-298 and different endocytosis compartments were labelled with different markers, including early endosome antigen-1 (EEA-1), late endosome (Rab7) and recycling endosome (Rab11), to study their colocalization. **Results:** The CD36 receptor is colocalized with early endosomes, reaching a plateau after 10 min of incubation with MPE-298. The results also show a colocalization with the late endosome marker Rab7 in the same time range. **Conclusion:** This study shows that binding of azapeptide MPE 298 to the membrane CD36 receptor induces rapid endocytosis of the MPE 298-CD36 complex in macrophages and that the internalized fluorescent tracer-labelled CD36 complex is rapidly accumulated in early and late endosomes following exposure of macrophages to azapeptide. The presence of labelled internalized CD36 in late endosomes suggests its potential transfer via multivesicular bodies to lysosomes.

### **Modulation of NAD(P)H:quinone oxidoreductase 1 by Methylmercury in Mouse Hepatoma Hepa1c1c7 cells**

Mohammed Alqahtani, Ayman El-Kadi

Pharmacy and Pharmaceutical Sciences, University of Alberta, Edmonton, Canada

**Purpose:** NAD(P)H:quinone oxidoreductase (NQO1)-mediated detoxification of quinones plays a key role in cancer prevention. Heavy metals typified by methyl mercury (MeHg) showed to alter the carcinogenicity of aryl hydrocarbon receptor ligands, mainly by modifying various xenobiotic-metabolizing enzymes such as NQO1. **Methods:** We examined the effect of MeHg on the expression of Nqo1 gene in mouse hepatoma hepa1c1c7 cells. For this purpose, Hepa1c1c7 cells were incubated with various concentrations of MeHg (1.25, 2, and 5  $\mu$ M) in the absence and presence of two Nqo1 inducers, 2,3,7,8-tetrachlorodibenzo-p-dioxin (TCDD) and isothiocyanate sulforaphane (SUL), as bifunctional and monofunctional inducers, respectively. **Results:** MeHg increased the expression of Nqo1 mRNA in a time-dependent manner. Furthermore, MeHg increased Nqo1 at the mRNA, protein, and activity levels in the presence and absence of both Nqo1 inducers, TCDD and SUL in a time-dependent manner. Moreover, these findings were coincided with increased nuclear accumulation of NQO1 transcription factor protein, nuclear factor-erythroid factor 2-related factor 2 (NRF2) indicating an involvement of a transcriptional modulation exhibited by MeHg. However, Nqo1 mRNA and protein decay experiments revealed a lack of posttranscriptional and posttranslational mechanisms. **Conclusion:** This study demonstrates that

the upregulation of Nqo1 gene expression by MeHg is possibly through a transcriptional mechanism in Hepa1c1c7 cells. Also NRF2 protein expression showed involvement in the modulation of Nqo1 by MeHg.

### **Towards a new era of vancomycin therapeutic monitoring: external evaluation of population pharmacokinetics models in pediatrics**

Mathieu Blouin,<sup>1</sup> Aysenur Yaliniz,<sup>2</sup> Marie-Élaine Métras,<sup>3</sup> Isabelle Viel-Thériault,<sup>4</sup> Julie Autmizguine,<sup>5</sup> Amélie Marsot,<sup>6</sup>

<sup>1</sup>Pharmaceutical Sciences, Université de Montréal, Laval; <sup>2</sup>Biopharmaceutical Sciences, Université de Montréal, Montreal; <sup>3</sup>Université de Montréal and CHU Sainte-Justine, Montreal; <sup>4</sup>Pediatrician, CHU de Québec-Université Laval, Quebec; <sup>5</sup>Pediatrician, Université de Montréal and CHU Sainte-Justine, Montreal; <sup>6</sup>Université de Montréal and CHU Sainte-Justine, Montreal, Canada

**Purpose:** Vancomycin, an antibiotic used to treat Gram-positive bacteria, has a narrow therapeutic index and large interindividual variability. After several years of therapeutic monitoring using trough concentration as a surrogate, the latest guidelines rather suggest the use of a population pharmacokinetics (popPK)-guided Bayesian approach to better assess vancomycin exposure. The aim of this study was to evaluate the predictive performance of pediatric vancomycin popPK models, use the most predictive one to develop an initial dosing nomogram and implement it in clinical practice at CHU Sainte-Justine. **Method:** An external database of 74 pediatric patients accounting for 263 vancomycin concentrations, allowed the evaluation of seven popPK models found in the literature (1, 2) up to December 31, 2021 Prediction errors (PE) were calculated as the relative difference between predicted concentration (NONMEM, v7.5) and the corresponding observed concentration Bias (median PE < +/- 20%) and imprecision (median |PE| < 30%) were considered for adequate predictive performance. **Results:** The study population has median values [range] of total body weight 13.0 [2.9-105.7] kg, age 3 [0-17] years old and serum creatinine 37.0 [17.2-73.0] µmol/L. All models had inadequate predictive performance based on the aforementioned criteria, so we re-estimated parameters and compared them to their initial values before calculating bias and imprecision de novo. After re-estimating parameters, five of the seven models showed adequate predictive performance. The model developed by De Cock et al (3) was the most predictive one with values of bias 3.2% and -1.8% for populational and individual data respectively, as well as imprecision 25.7% and 13.2% for populational and individual data respectively. **Conclusion:** After re-estimating parameters, the popPK model initially developed by De Cock et al (3) showed the best predictive performance. It can be used to develop an initial dosing nomogram and to assess vancomycin exposure with a Bayesian approach.

### **Development of Liver Microsomal and Cytosolic Scaling Factors For Female Yucatan Minipigs**

Austin Zimmer, Michael Doerksen, Abby Collier

The University of British Columbia, Vancouver, Canada

**Purpose:** In vitro-in vivo extrapolation (IVIVE) utilizes biochemical studies of in vitro metabolism, along with mathematical modelling, to help predict whole animal and human clearance. Central to hepatic IVIVE are the scaling factors, microsomal protein per gram of liver (MPPGL) and cytosolic protein per gram of liver (CPPGL), given the abundance of drug metabolizing enzymes in both cellular fractions MPPGL and CPPGL scalars are undefined for the minipig, which is used in many preclinical pharmacology studies. **Methods:** Samples (n=4) were harvested from whole liver and flash frozen. When ready, samples were thawed, wet weigh recorded, and homogenized in Sucrose-HEPES Differential centrifugation (10,000x g, then 100,000x g) isolated microsomal and cytosolic fractions Fraction protein content was quantified, and scalars subsequently derived. Microsomal intactness was quantified by means of mannose-6-phosphatase assay. The effect of freeze thaw cycling (n=3) on

protein content was measured using a BCA and Bradford assay to investigate variation in scalar values. Results: Mean MPPGL and CPPGL values of  $24.3 \pm 3.2$  mg protein/g liver, and  $75.6 \pm 1.42$  mg protein/g liver were derived. Mean microsomal intactness was  $74.8 \pm 7.6\%$ , indicating good integrity Freeze thaw effects were determined for n=1 cycles (MPPGL:  $19.2 \pm 2.8$  mg protein/g liver CPPGL:  $66.8 \pm 9.8$  mg protein/g liver), n=2 (MPPGL:  $19.7 \pm 1.8$  mg protein/g liver CPPGL:  $64.6 \pm 7.9$  mg protein/g liver) and n=3 (MPPGL:  $18.4 \pm 2.8$  mg protein/g liver CPPGL:  $5.94 \pm 10.7$  mg protein/g liver). All  $p < 0.05$  excluding n=1 for CPPGL. Conclusion: Here we have derived MPPGL and CPPGL scalars for the female Yucatan minipig. We have additionally demonstrated that scalar values are highly sensitive to freeze thaw effects Since protein levels decline, indicating degradation; use of microsomes and cytosol should be within 1 freeze thaw cycle.

\*\*\*